UiT The Arctic University of Norway

Faculty of Biosciences, Fisheries and Economics
Department of Arctic and Marine Biology

Snow depth effects on vegetation dynamics and development of near-remote sensing techniques in high-Arctic tundra

Andreas Jørgensen
Master's thesis in Biology BIO-3950 May 2022

Snow depth effects on vegetation dynamics and development of near-remote sensing techniques in high-Arctic tundra

Andreas Jørgensen
Master's thesis in Biology BIO-3950 May 2022

Supervisors

Elisabeth Cooper, UiT – The Arctic University of Norway

Lennart Nilsen, UiT – The Arctic University of Norway

Cover photograph: © Agnes Nielsen – *Cassiope tetragona* in Adventdalen

Table of Contents

List of Tables

List of Figures

Acknowledgements

I would like to thank everyone who has helped and supported me in my thesis work.
First, I would like to thank Elisabeth Cooper and Lennart Nilsen for their dedicated supervision throughout my thesis. Thank you for traveling to Svalbard and helping me in the field, for our countless meetings and discussions, and for your positivity and encouragement throughout my thesis work. It has been a pleasure to work with you both.

I would not have been able to complete my field work without the financial support I received from The Research Council of Norway through their Arctic Field Grant, nor without the financial and logistical support I received from the Korea Polar Research Institute. Thank you to Dr. Yoo Kyung Lee for collaboration in the field.

I am grateful to Agnes Nielsen and Kaspar Lehnert who assisted me on long days in the field. Thank you for all your hard work, and for a great time in Svalbard. Also, thank you to Simone Lange and the University Centre in Svalbard for kindly letting me borrow field equipment.

I had helpful discussions about my statistical analyses with Nigel Yoccoz, Phillip Semenchuk, Martin Mörsdorf, and Mikel Armendariz. Thank you for your ideas and inputs.

I am grateful for the encouragement and support I have received from friends and family throughout this time, especially from my parents. And finally, thank you Anna for being there for me every single day. Having you by my side to help and motivate me through this process has been amazing. Thank you for sharing all those hours with me working on our theses together and for exploring the wilderness with me on our many trips. It all means a lot to me.

Abstract

Snow exerts key controls on many aspects of plant ecology in the Arctic, including community composition. With climate predictions forecasting dramatic changes in winter climate and snow cover in the Arctic in the near future, it is important to improve our understanding of snow effects on plant communities in these regions. This study used a snow depth manipulation experiment established in 2006 in Adventdalen, Svalbard, Norway (78°10'N, 16°04'E) to investigate long-term effects of deepened snow on plant community composition. Two common tundra vegetation types were studied (*Cassiope* heath and mesic meadow) using data from three years (2015, 2020, and 2021). The study further used 'near-remotely' sensed vegetation indices (VIs; RGB-based indices, image based, and non-image based NDVI) to describe differences between snow regimes, years, and vegetation types. Green Chromatic Coordinate as well as image and non-image based NDVI were compared with cover of major plant groups in an initial step towards understanding the relationships between VIs and plant cover over several years and in different vegetation types. This study documented general decreases in the cover of live vascular plants, especially shrubs, and simultaneous increases in bryophytes and the forb *Bistorta vivipara* under deepened snow. Community changes were similar between the Heath and the Meadow vegetation types but changes were more pronounced in Heath. Near-remotely sensed VIs showed differences between snow regimes, possibly reflecting the documented vegetation change. However, relationships between VIs and plant cover were ambiguous when compared between years, vegetation types and snow regimes. The relationships generally differed in magnitude, but sometimes also direction, and were likely confounded by phenology and variations in maximum VI values between years. These findings highlight remaining challenges in the use of near-remote sensing as a tool for vegetation monitoring. Further studies should investigate the relationships between VIs and plant cover in a context of annual variations in maximum VI values, and phenological stages, as this may improve the usefulness of near-remote sensing in the future.

Keywords: Winter climate change, snow depth, plant community composition, near-remote sensing, vegetation indices, Svalbard

1 Introduction

With climate change proceeding at its current rate in the Arctic, it is inevitable that snow conditions will be affected in the future (Bintanja & Andry, 2017). The most recent climate forecasts now suggest increasingly warming winters with more rain precipitation, shorter duration of snow cover and earlier spring-time snowmelt throughout the Arctic (Constable et al., 2022), including on Svalbard (Hanssen-Bauer et al., 2019). However, regional variation is expected, and snow depth may increase in some regions despite earlier snowmelt (Lemke et al., 2007).

Snow is known to play a major role as a modulator of ecosystem processes, especially in high-Arctic areas (Bokhorst et al., 2016; Callaghan et al., 2011), such as Svalbard, where snow cover can last for more than eight months of the year. Snow conditions have been shown to affect several aspects of plant ecology in the Arctic including community composition (Cooper et al., 2019; Happonen et al., 2019), species distributions (Niittynen & Luoto, 2018), soil and plant chemistry (Semenchuk et al., 2015, Mörsdorf et al., 2019), plant phenology (Bjorkman et al., 2015; Semenchuk et al., 2016), plant growth (Rumpf et al., 2014), and reproductive success (Cooper et al., 2011; Ellebjerg et al., 2008; Semenchuk et al., 2016). Indeed, snow conditions have been identified as the single most important control on plant community composition, with greater effect than summer air temperatures (Happonen et al., 2019; Wahren et al., 2005), and shorter snow cover duration has been shown to potentially act as a major driver of species extinctions and biodiversity loss in the Arctic (Niittynen et al., 2018).

The effects of snow on vegetation appear to be related to key properties of the snowpack such as snow depth and snow cover duration (Cooper, 2014; Niittynen et al., 2018; Niittynen & Luoto, 2018; Rixen et al., 2022) as these properties inherently affect local abiotic conditions and biogeochemical processes well into the snow-free summer period (Barichivich et al., 2014; Mörsdorf et al., 2019). Thick snow cover acts as an insulator with a positive effect on soil temperature (Pattison & Welker, 2014) which, in turn, lead to a greater depth of thaw as well as higher microbial activity, faster nutrient turnover (Edwards et al., 2007) and litter decomposition rates (Baptist et al., 2010). These effects are accompanied by increased soil moisture due to melting of the thicker snowpack, increasing both the quantities of plant available water (Barichivich et al., 2014; Johansson et al., 2013) and nutrients well into the

growing season (Mörsdorf et al., 2019; Xu et al., 2021). Furthermore, snow cover duration, and thus the timing of snowmelt, is a major factor determining the potential growing season length available for plant development, growth, and reproduction in summer.

Our understanding of snow effects on tundra communities is to a great extent based on snow depth manipulation experiments, often using snow fences or open top chambers to create an experimentally deepened snow treatment with paired control plots (Cooper et al., 2019; Rixen et al., 2022; Wipf & Rixen, 2010). The effects of snow on vegetation in such experiments are therefore related to snow depth in winter and also to later spring-time snowmelt since the thicker snowpack melts out later. Snow manipulation experiments have been carried out in several tundra locations, both in alpine (Mark et al., 2015; and see Wipf & Rixen, 2010), and Arctic sites including in North Amerika (Christiansen et al., 2018; Leffler et al., 2016; Natali et al., 2012; Wahren et al., 2005) and Phenoscandia (Johansson et al., 2013). The only high-Arctic snow manipulation site, to my knowledge, is located in Svalbard, Norway (Cooper et al., 2019; Mörsdorf & Cooper, 2021). Helpful overviews of known alpine and Arctic snow manipulation studies on vegetation composition and their main findings are provided in Mörsdorf & Cooper (2021) and Wipf & Rixen (2010).

Snow manipulation studies have found diverse responses in plant community composition to deepened snow, apparently depending on the experimental setting and geographical location (see Rixen et al., 2022). Evergreen shrubs have been found to increase in Daring Lake, Canada (Christiansen et al., 2018) but decrease in Toolik Lake, Alaska, USA, and Adventdalen, Svalbard, Norway (Cooper et al., 2019; Wahren et al., 2005). Deciduous shrubs increased in Toolik Lake (Leffler et al., 2016; Wahren et al., 2005) but decreased in Adventdalen (Cooper et al., 2019). Graminoids increased in Abisko, Sweden, and Daring Lake (Johansson et al., 2013; Natali et al., 2012) but decreased in Toolik Lake and Adventdalen (Cooper et al., 2019; Leffler et al., 2016). Bryophytes increased in Toolik Lake and Adventdalen (Cooper et al., 2019; Wahren et al., 2005) but not in Abisko or Daring Lake (Johansson et al., 2013; Natali et al., 2012). In Toolik Lake, contrasting responses in species diversity and shrub abundance were demonstrated between two vegetation types (moist tussock tundra and dry tundra) after 8 years of experimentally deepened snow (Wahren et al., 2005). In Adventdalen, declining shrub- and increasing bryophyte abundance was documented after 9 years of deepened snow, but magnitudes of these responses were different

between a heath and a meadow vegetation type (Mörsdorf & Cooper, 2021). The diversity of the outlined findings show that tundra communities are responding to climate change, and especially changes in snow conditions, in a highly heterogeneous way (see also Elmendorf et al., 2012), and most likely are influenced greatly by the amount of snow in ambient/experimental conditions, soil moisture content, and vegetation types under effect (Cooper et al., 2019, Mörsdorf & Cooper, 2021, Rixen et al., 2022).

It is clear that the role of snow in shaping Arctic tundra plant communities is a research area which requires further investigation, and which would greatly benefit from additional long-term studies. However, long-term, field-based vegetation monitoring can be challenging in Arctic areas, such as Svalbard, where field campaigns are costly and work often must be done in remote locations and challenging conditions. For this purpose, remote sensing is an extremely helpful tool for obtaining data with good spatiotemporal coverage. However, the coarse scale of satellite based remote sensing data is a fundamental, yet unresolved, issue in using satellite data to describe and understand vegetation dynamics at the much finer spatial scale on which we can expect snowpack to affect vegetation (Parmentier et al., 2021). Thus, much ground truthing has yet to be done in order to reliably use satellite data for this purpose in Arctic regions (Beamish et al., 2020; Myers-Smith et al., 2020; Pan et al., 2018). It has also been pointed out that satellite data with good temporal coverage can be largely unobtainable in heavily clouded regions of the Arctic such as Svalbard (Karlsen et al., 2018).

As a method for ground truthing, and for inexpensively obtaining ground-level data on vegetation dynamics (including community composition, phenology and net productivity), near-remote sensing techniques have received increasing attention in recent years (Anderson et al., 2016, 2017; Cooper et al., 2019; Parmentier et al., 2021; Peter et al., 2018; Westergaard-Nielsen et al., 2013, 2017). These studies have further focused on the use of inexpensive RGB (Red-Green-Blue) cameras (i.e., normal digital cameras) as an alternative to the more costly near-infrared (NIR) sensors or RGN (Red-Green-NIR) cameras needed to obtain the widely used Normalized Difference Vegetation Index (NDVI). Several RGB-based vegetation indices (VIs), including Green Chromatic Coordinate (GCC; also known as Channel_G%), 2G_RBi, and Green-Red vegetation index (GRVI), have been used to identify phenological stages in common vegetation types in Svalbard (Anderson et al., 2016, 2017). The RGB-based ‘Excess Green’ index (ExG; also referred to as GEI) and NDVI (from

handheld, non-imaging sensors) have been used to describe vegetation composition in the Arctic (Beamish et al., 2016; Cooper et al., 2019). However, whether near-remotely sensed NDVI or RGB-based VIs can be used to describe temporal variation in community composition over several years remains untested.

This study aims at advancing our understanding of the usefulness of near-remote sensing as a tool for describing vegetation change in Arctic tundra. This study also aims at illuminating the effects of snow depth on plant community composition in two vegetation types, by using data from a 15 year-running snow fence experiment in Adventdalen, Svalbard. Specifically I aim to:

1) Describe overall observed year-to-year changes in plant community composition in plots with experimentally deepened snow (*Deep*) and control plots (*Ambient*) in two vegetation types (Heath and Meadow), using data from 2015, 2020 and 2021. It is expected that, in accordance with Cooper et al. (2019):
    a. Dwarf shrub cover decreased while bryophyte cover increased in *Deep* plots.
    b. Dead plant material increased in *Deep* plots, especially from dwarf shrubs.

    It is further expected that:
    c. Any effects of deepened snow on plant cover got larger over time.
2) Test several RGB image based VIs (Excess Green, Greenness Index, Green Chromatic Coordinate, and 2G_RBi) as well as NDVI (image and non-image based) for overall differences between *Deep* and *Ambient* snow regimes, and between Heath and Meadow vegetation types, in 2015, 2020, and 2021. Further, the relationships between a subset of VIs (Green Chromatic Coordinate, image and non-image based NDVI) and plant species/functional group cover will be explored. It is expected that:
    a. Vegetation indices differ between *Ambient* and *Deep* snow regimes as well as between Heath and Meadow vegetation types. It is further expected that VIs reflect changes in plant community composition over the study period.
    b. One or more VIs will correlate with cover of major plant species and/or functional groups, and reflect changes in these between 2015, 2020 and 2021.
3) Use the knowledge obtained in point 2 to evaluate the suitability of near-remote sensing technology (imaging and non-imaging) for describing and monitoring vegetation change in the future.

2 Methods

2.1 Study site

The study site is located in Adventdalen, Svalbard, Norway (78°10'N, 16°04'E), a large valley in the western part of Spitsbergen. This high-Arctic valley has a mean annual temperature of -4.7 ± 1.9 °C (from 1976-2020; data available from Svalbard Airport about 15 km west of the study site at seklima.met.no). Summer temperatures are cold, with mean July temperatures at 6.9 ± 1.1 °C (1976-2020), and the growing season is as short as six to ten weeks for most plants (Semenchuk et al., 2016). Mean annual precipitation in the same years was 196.2 ± 46.0 mm with most of this precipitation falling as snow in the winter. The valley is underlain by permafrost throughout, and the active soil layer thickness within the study site was only 91.1 ± 18.7 cm by mid-August 2021 (own data, unpublished). Maximum active soil layer thickness was measured at the site in 2012 by Xu et al. (2021), where it was between 106-130 cm depending on vegetation type and snow regime.

The vegetation within the study site is characteristically Arctic with very little vegetation above 10 cm in height and few species present. Valleys in the central Spitsbergen are generally dominated by two major vegetation types; *Cassiope* heath and mesic meadow (Elvebakk, 2005). *Cassiope* heaths beneath the rocky valley slopes are dominated by the evergreen dwarf shrub *Cassiope tetragona* L. while other common vascular plants include *Dryas octopetala* L., *Salix polaris* Wahlenb., *Alopecurus ovatus* Knapp. and *Bistorta vivipara* L. (Cooper et al., 2011; Morgner et al., 2010). The landscape topography is varied with many ridges and hollows, but the study locations were established in flat to gently north-facing, sloping areas. The soil is stony and relatively well-drained with a continuous moisture supply throughout the growing season (Elvebakk, 2005; Morgner et al., 2010). Mesic meadows contain many of the same plant species as *Cassiope* heath but are generally dominated by *S. polaris* while *Luzula confusa* Lindeb., *A. ovatus, D. octopetala* and *B. vivipara* are also abundant (Cooper et al., 2011). *Cassiope tetragona* grows in smaller patches. Other common species across the study area include: *Oxyria digyna* L., *Stellaria longipes* Goldie., *Pedicularis hirsuta* L., and *Equisetum arvense* L. spp. *Alpestre* Wahlenb. Bryophyte cover is greater in mesic meadows compared to *Cassiope* heath and can often constitute up to 50% or more of the plant cover. The most common bryophytes are *Sanionia uncinata* Hedw., *Tomentyphnum nitens* Hedw., *Polytrichum* Hedw. spp., *Dicranium* Hedw. spp., and

Distichium Bruch & Schimp spp. (Cooper et al., 2019). Common lichens include *Rhizocarpon geographicum* L., *Stereocaulon* Hoffm. spp., *Thamnolia vermicularis* Sw. and *Cetrariella delisei* Bory ex Schaer. The meadows are situated further away from the valley sides, on flat river terraces with a fine and mesic soil created by fluvial deposits. In some places these river terraces are disturbed by cryoturbation. The scientific names for vascular plants are according to the PanArctic-Flora (panarcticflora.org).

2.2 Experimental design

This study was conducted within a long-term field experiment established in 2006, using snow fences to modify snow depth (Morgner et al., 2010). The fences were 6 m wide and 1.5 m tall. They were placed perpendicular to the dominant wind direction which is south-easterly in the valley (Figure 1-2). This simple design causes drifting snow to accumulate on the leeside of the fences where snow depth increases in an area of > 20 m behind the fence (Cooper et al., 2011). The snow is deepest in the area of 3-12 m behind the fence, hereafter called '*Deep'* snow regime; where the maximum winter snow depth is up to 1.2 m greater than *Ambient* snow depth (Morgner et al., 2010; Figure 1-2).

Twelve snow fences were established in 2006 in a multi-factorial, nested design. Six fences were placed in each of the two major vegetation types in the valley; *Cassiope* heath and mesic meadow (from here; 'Heath' and 'Meadow'). Two separate clusters of three snow fences (hereafter 'blocks') were placed in each of the vegetation types (blocks A-B in Heath and C-D in Meadow). Each block was about 200 x 200 m and all blocks were located within an area of about 2.5 x 1.5 km with a minimum distance of 500 m between the blocks (Figure 3). At each fence location, six vegetation plots (75 x75 cm) were placed in the *Deep* snow regime as well as six plots in the *Ambient* snow regime. *Ambient* plots served as control plots for each fence, and were placed to the side of the fence, on areas checked to be unaffected by snow melting from the fences. Of the six plots in each snow regime (*Deep* or *Ambient*), three were placed such that the dominant evergreen dwarf shrub (DES) was *Dryas octopetala,* and three such that *Cassiope tetragona* was the DES (from here; '*Dryas'* and '*Cassiope'* plots). One snow fence (fence *C8*) did not have any *Cassiope* plants and therefore no *Cassiope* plots in the *Deep* snow regime. Thus, only the three *Dryas* plots were included as *Deep* plots at this fence. One fence (fence *A2*) collapsed before 2015, and therefore no plots associated with that fence were used in this study. The river terraces are subject to dramatic permafrost-driven soil

movement, and in some areas large-scale soil collapses are visible, which occurred after the establishment of the site. This is especially notable in one area where an ice lens has possibly collapsed and left a large, ~1.5 m deep, water-filled crater in the ground behind a snow fence (fence C7; Parmentier et al., 2019; and see Figure S1). This fence was still included in the study although two plots which were completely submerged in water were not surveyed. Thus, this study includes the survey of 127 permanent plots (Table 1) from 11 fence locations. The plots were established in 2007 and data for this study was collected in 2015, 2020 and 2021.

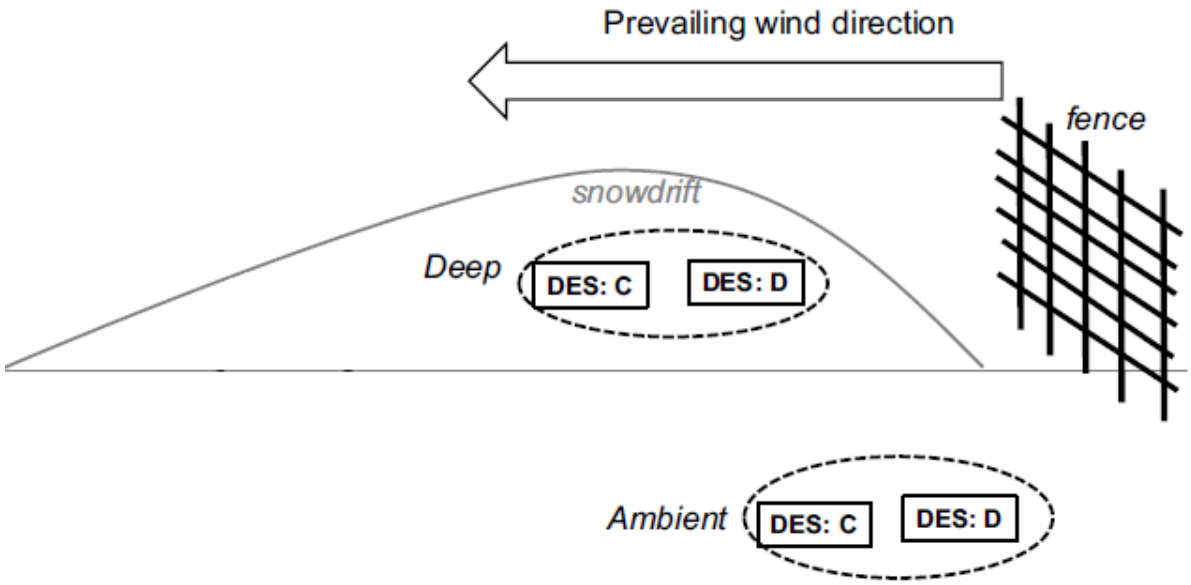

Figure 1. Schematic drawing of a snow fence and location of plots. Prevailing wind direction causes deposition of a snow drift behind the fence. In the area of 3-12 m behind the fence, snow depth is ~1 m deeper than the ambient snow depth. 'Deep' plots are placed in this area of deepened snow while 'Ambient' plots are placed to the side of the snow fence to serve as control plots for the 'Deep' treatment. Dominant Evergreen Shrub (DES) was assigned; three plots with Cassiope tetragona (C) and three plots with Dryas octopetala (D). Redrawn after Cooper et al. (2019).

Figure 2. Accumulation of snow behind fence resulted in deepened snow and later snowmelt. Photograph from Cooper et al. (2011).

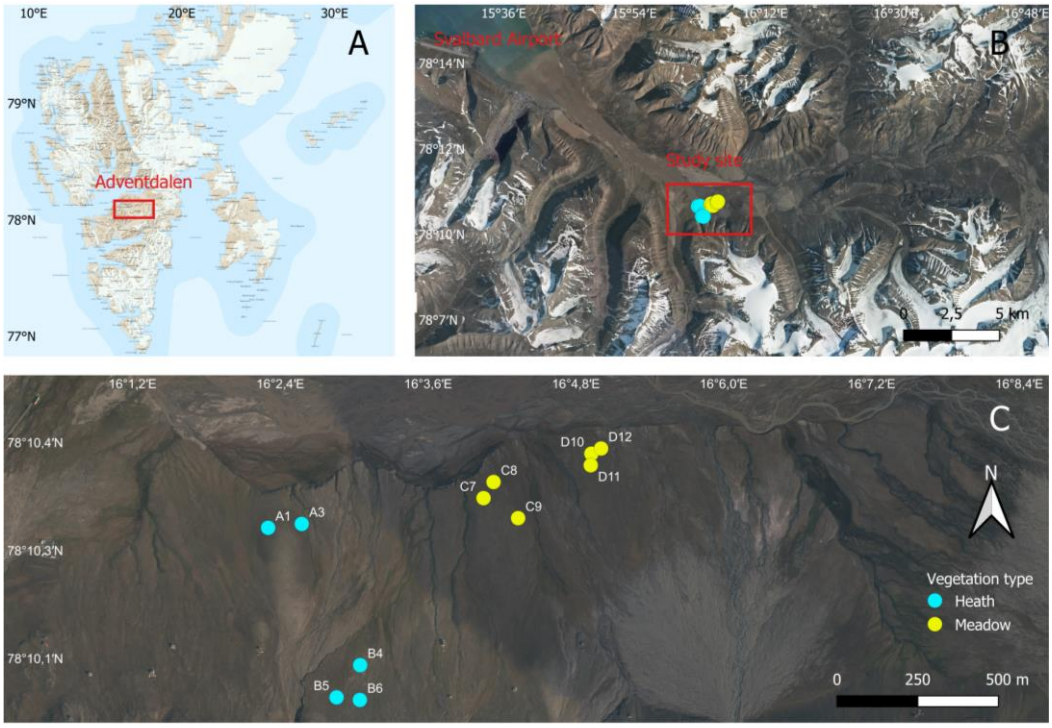

Figure 3. Map of the study area. A: Location of Adventdalen, Svalbard. B: Location of the study site and Svalbard Airport within Adventdalen. C: Location of 11 snow fences within the study site. Fence A2 collapsed before 2015 and was therefore not used in this study. Snow fences are nested into four 'Blocks', indicated with capital letters A-D. Blocks A and B are in Heath while blocks C and D are in Meadow vegetation. Map and orthophotos accessed at geodata.npolar.no.

2.3 Data collection

Data collection consisted of making ground cover estimates, photographing, and measuring NDVI, at the permanent plots at peak-growing season (mid-July to early August) in 2015, 2020 and 2021 (Table 2; Figure 4). In 2015, a subset of 39 plots was surveyed while all 127 plots were surveyed in 2020 and 2021. All 2021 data was collected in the field by myself while data from previous years was collected by other scientists.

Table 1. Number of plots included in the categories 'Snow Regime' (Ambient or Deep), 'Dominant Evergreen Shrub' (Cassiope or Dryas) and 'Vegetation Type' (Heath or Meadow). Numbers indicate plots surveyed in 2020 and 2021 while numbers in parentheses indicate plots surveyed in 2015. Total number of plots surveyed in 2020 and 2021 was 127. Thirty-nine (39) plots were included in 2015.

Snow Regime	Dominant Evergreen Shrub	Heath	Meadow	Sum
Ambient	*Cassiope*	15 (5)	18 (5)	33 (10)
	Dryas	15 (5)	18 (5)	33 (10)
Deep	*Cassiope*	15 (5)	15 (4)	30 (9)
	Dryas	15 (5)	16 (5)	31 (10)

Table 2. Dates for data collection in year 2015, 2020 and 2021 as well as time of snowmelt and thawing degree days (TDD; temperature sum of days with mean temperature > 0°C since snowmelt) at the first day of ground cover data collection and photograph collection. Mean monthly temperature between June-August are also shown for each year. Number of plots used in the respective years (n) is indicated in parenthesis. Dates given as Day of Year (DoY). Climatic data obtained from Svalbard Airport, 15 km West of the study site (data available at seklima.met.no).

Year	Jun-Aug temperature (mean; °C)	Snowmelt (DoY)	Ground cover (DoY)	Ground cover (TDD)	Photographs (DoY)	Photographs (TDD)
2015 (*n = 39*)	6.7	138	215-219	348.7	198-204	255.9
2020 (*n = 127*)	7.1	113	198-206	296.2	198-206	296.2
2021 (*n = 127*)	5.2	154	197-202	109.5	197-202	109.5

2.3.1 Ground cover estimates

Ground cover was obtained for a list of predetermined individual plant species, genera, and functional groups. This was done by visually estimating the per cent of ground covered by each plant or category in the permanent vegetation plot of 75 x 75 cm (Figure 4). Per cent ground cover was also estimated for the non-vegetated proportion of each plot (Table 3). The total ground cover for a plot always summed to 100%. Ground covers were subjective estimates made by observers in the field. To mitigate potential observer bias, estimates were usually carried out by two observers working together to increase accuracy, but sometimes plots were observed only by one observer for efficiency.

Table 3. Categories (first column) for which ground cover was estimated in each plot in 2015 (n = 39), 2020 (n = 127), and 2021 (n = 127). Note that the sum of all these categories equals 100% in each vegetation plot. Combined categories which were subsequently used in the analyses are indicated on the right side of the table. 'X' indicates that a plant was included in the given category. 'Vascular plants' and 'Shrubs' and were divided into subcategories; 'Live vascular plants', 'Dead vascular plants', 'Live shrubs' and 'Dead shrubs'. 'Live graminoids' included live plant material only. 'Total live plants' included live vascular plants and bryophytes, but no distinction could be made between dead and live bryophytes.

	Combined categories used in analysis			
All surveyed ground cover categories	Total live plants	Live/dead vascular plants	Live graminoids	Live/dead shrubs
Cassiope tetragona	X	X		X
Dryas octopetala	X	X		X
Salix polaris	X	X		X
Bistorta vivipara	X	X		
Pedicularis spp.	X	X		
Alopecurus ovatus	X	X	X	
Luzula spp.	X	X	X	
Other graminoids	X	X	X	
Other plants: herbs and *Equisetum*	X	X		
Bryophytes	X			
Lichens				
Soil and biocrust				

The surveyed plants included separate dead and live cover of the following vascular plants: *C. tetragona*, *D. octopetala*, *S. polaris*, *B. vivipara*, *Pedicularis* spp., *A. ovatus*, *Luzula* spp., and 'other graminoids'. The genus *Pedicularis* was represented by the two species *P. dasyantha and P. hirsuta* but no distinction was made between these. The *Luzula* genus was similarly represented by two species between which no distinction was made; *L. confusa* and *L. nivalis.* Dead and live cover was also observed separately for the category 'other plants' which consisted of forbs in the genera *Oxyria* L., *Saxifraga* L., *Micranthes* Haw., *Draba* L., *Papaver* L., *Stellaria* L., and *Cerastium* L. as well as a single species of horsetail; *Equisetum arvensis* spp. *alpestre.* Surveyed cryptogams included bryophytes and lichens, and no discrimination was made between dead and live material of these categories. A combined category ('soil & biocrust) was also included for biological crust (including cyanobacteria), bare soil, animal droppings and stones. Ground cover data was collected using the same methodology each year, by different field workers but with training and guidance from the same project leader.

2.3.2 Vegetation indices

Normal RGB (Red-Green-Blue) photographs were taken of each plot during peak-growth in mid-July in all three years (Table 2; Figure 4). All photographs were taken with normal digital cameras with autofocus and an automatic setting for shutter speed, aperture, and ISO. Different cameras were used each year (*Ricoh Digital 3*, *Sony Ilce-6100*, *Canon Powershot G16* in 2015, 2020 and 2021, respectively). The same plots were used for photographs as for ground cover. Additionally, in 2021 all plots were photographed with a MAPIR 3 RGN (Red-Green-NIR) camera (MAPIR, San Diego, CA, USA). The cameras were mounted on an aluminium frame (75 x 75 cm) with the camera fixed at 150 cm above ground, lens pointing vertically towards the ground (Figure 4). In addition to the image-derived VIs, a 'GreenSeeker' handheld, non-imaging crop-sensor (Trimble Agriculture, Westminster, CO, USA) was used to measure NDVI in all plots in all three years. This sensor is an active sensor (as opposed to passive, imaging sensors), meaning that measurements are obtained by sending out red and near-infrared radiation, and subsequently measuring the radiation which is reflected by the vegetation. In 2020-2021, NDVI was measured with the GreenSeeker on the same days as ground cover estimates were made, with the sensor held at 90 cm above the ground. Three measurements were done per plot, and the mean value used in the statistical

analysis. In 2015, NDVI was measured in the same way on July 15 and 22 (DoY 197 and 204). For the statistical analysis, mean value between these dates was used.

2.4 Image data processing

From RGB images the following VIs were derived: Green Chromatic Coordinate (GCC), Excess Green (ExG), 2G_RBi, and Greenness Index (GI). Normalized Differences Vegetation Index (NDVI) was derived from the MAPIR 3 RGN images for each plot in 2021. All MAPIR images were calibrated prior to processing, using the standard calibration option in MAPIR Camera Control (MCC) version 10/16/2019, an open-source software made available by the camera manufacturer (MAPIR, Inc. (2019). MCC. www.mapir.camera/collections/software). NDVI obtained with the GreenSeeker did not require any processing before analysis.

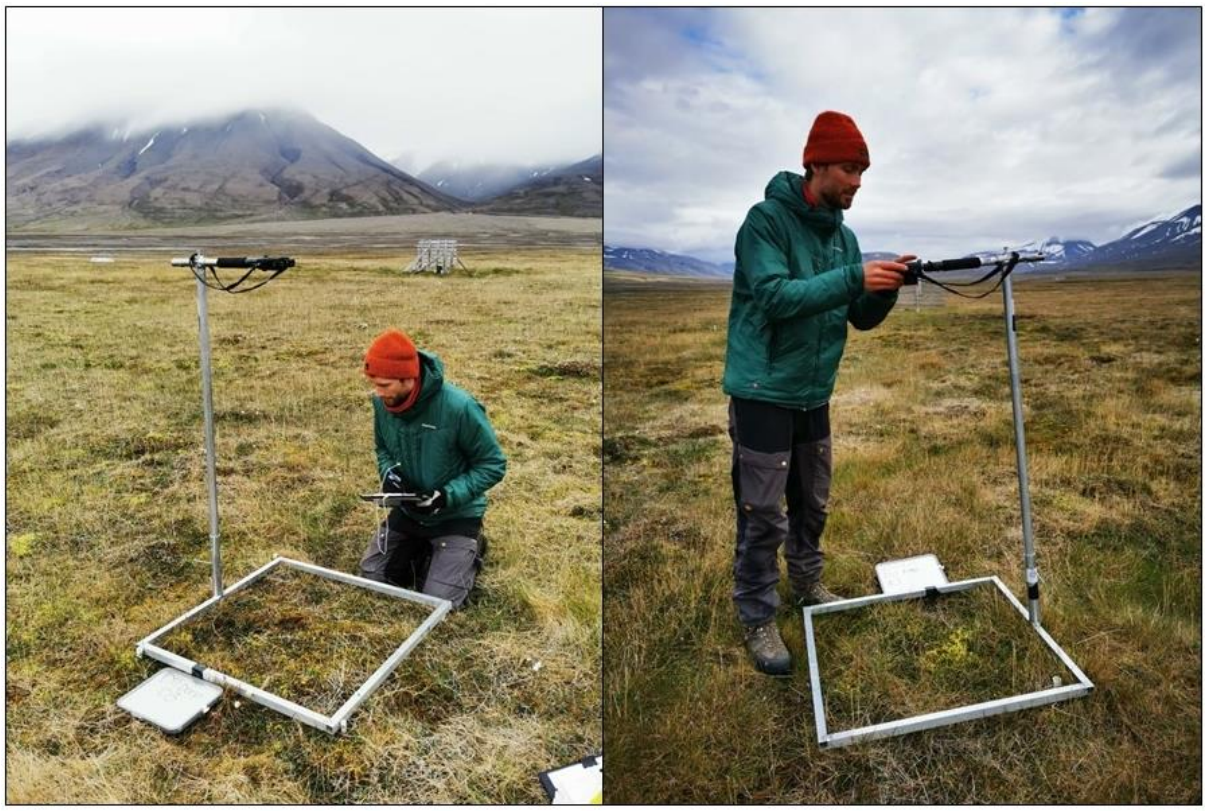

Figure 4. Photos from field work in 2021. Left: Myself doing visual ground cover estimate for a plot in the 'Ambient' snow regime in Meadow using a 75 x 75 cm frame to delineate the plot. Paired snow fence visible in the background. Right: Using the frame with mounted RGB camera to photograph a plot. RGB images were later used for calculation of RGB-based vegetation indices.

Figure 5. Example of a plot photograph taken with an RGB camara mounted 1.5 m above ground with a 75 x 75 cm aluminium frame. The frame and surrounding vegetation were cropped out before vegetation indices were extracted from the image. White flowers in the plot belong to the shrub Cassiope tetragona.

Table 4. Formulas for calculation of vegetation indices. RDN, GDN, BDN and NIRDN: digital number of pixels in red, green, blue and near-infrared bands. nR, nG and nB: normalised digital numbers of red, green and blue bands as respective bands divided by (RDN + GDN + BDN).

Vegetation index	**Formula**
RGB-based indices	
Green chromatic coordinate (GCC)	$GCC = \frac{G_{DN}}{R_{DN} + G_{DN} + B_{DN}}$
2G_RBi	$2G\_RBi = 2G_{DN} - (R_{DN} + B_{DN})$
Greenness index (GI)	$GI = \frac{2G_{DN} - (R_{DN} + B_{DN})}{2G_{DN} + (R_{DN} + B_{DN})}$
Excess Green (ExG)	$ExG = 2nG - (nR + nB)$
Excess Green-Red (ExGR)	$ExGR = ExG - 1.4nR - nG$
Green-Red Vegetation Index (GRVI)	$GRVI = \frac{G_{DN} - R_{DN}}{G_{DN} + R_{DN}}$
NIR based indices	
Normalized differences vegetation index (NDVI)	$NDVI = \frac{NIR_{DN} - R_{DN}}{NIR_{DN} + R_{DN}}$

It was necessary to crop all RGB and RGN images in order to standardize the plot area, and exclude the aluminium frame and vegetation surrounding the plot before extracting VIs. This was done using the open-source photo-editing software GIMP version 2.10.22 (The GIMP Development Team. (2019). GIMP. https://www.gimp.org). RGB and RGN images were imported as JPEG-format, cropped using the 'Free selection' tool, and exported in uncompressed TIF-format (Figure 5). Vegetation indices were then extracted from the TIF-files in RStudio (RStudio Team, 2022), using the 'raster'-package (Hijmans, 2022). Digital numbers were extracted for the red, green, and blue channels in the case of RGB images, and for the red and near-infrared (NIR) channels in the case of RGN images. The values of the respective VIs were then calculated for each pixel according to the equations given in Table 4 and summarized to a mean value for each VI in all plots.

2.5 Statistical analysis

Prior to the statistical analyses, a thorough data exploration was conducted as recommended by Zuur et al. (2010) and Zuur & Ieno (2016) to avoid problems with violation of underlying assumptions in the statistical approach. The data was investigated for the presence of outliers, collinearity among covariates and heteroscedasticity. The data exploration led to the exclusion of all plots which contained water, as water severely impacted the VIs and led to the presence of true outliers in the dataset. This meant that four plots were excluded from the statistical analyses in year 2020 and 2021. Thus, the data used in those years included 123 plots for all analyses. Plot identifiers for all plots which were included in the statistical analyses are listed in Table S2. All statistical analyses as well as data exploration were carried out in RStudio (RStudio Team, 2022).

2.5.1 Effect of snow regime, vegetation type, and year on community composition

A distance-based redundancy analysis (dbRDA; Legendre & Anderson, 1999) was conducted using the 'capscale'-function of the 'vegan'-package in R (Oksanen et al., 2020). This constrained ordination method allowed for explicitly investigating the effects of snow regime (*Ambient* or *Deep*), vegetation type (Heath or Meadow) and year (2015, 2020 or 2021) on plant community composition, including relative abundances of plants, as well as testing for multivariate interactions. The method further allowed 'partialling out' any variance described by the variables *'Fence'* (denominating fence location) and *'Dominant Evergreen Shrub*

(DES)', similar to using random effects in linear mixed-effects modelling. This was done to account for spatial variability between the 11 snow fences as well as the inherent variability in *Dryas* and *Cassiope* cover described by '*DES*'. A significant advantage of the dbRDA is that it allowed for the use of the non-Euclidean Bray-Curtis distance, a good measure of ecological distance for species abundance data (Faith et al., 1987; Legendre & Legendre, 2012). The use of Bray-Curtis distances further prevented double-zeros effects, where the absence of the same species in two different plots unduly influences the ecological distance between those plots. Significance of the terms *'Snow regime', 'Vegetation type', 'Year'* and the interactions *'Snow regime × Year'* and *'Snow regime × Vegetation type'* was assessed through permutation tests using 999 permutations. Further, a model selection was run in which different combinations of significant model terms were compared by both an Akaike Information Criterion (AIC)-like criterion based on Chi-squares, as well as by adjusted R^2-values (Table S1). This was done by applying the 'ordistep'- and 'ordiR2step'-functions of the 'vegan'-package with a forward selection and 999 permutations.

2.5.2 Effect of snow regime, vegetation type, and year on cover of individual plant species/functional groups

The relationship between plant cover and snow regime (*Ambient* or *Deep*), vegetation type (Heath or Meadow), and year-to-year variation between 2015, 2020 and 2021 was examined for a selection of plant species and functional groups (see Table 3). These were live *Cassiope*, live *Dryas*, live *Salix*, live *Bistorta*, live shrubs, live graminoids, total live vascular plants, total live plants, bryophytes, lichens, as well as total dead vascular plants, dead shrubs, and soil & biocrust (including stone and faeces). For this purpose, Generalized Linear Mixed-effects Models (GLMMs) were applied for each category, resulting in 13 separate GLMMs. All GLMMs were done using the 'glmmTMB'-package in R (Brooks et al., 2017).

Since the ground cover data was proportional and had zero-truncated distributions, these models were done by applying GLMMs with beta-distributions and logit link-functions as recommended by Damgaard & Irvine (2019). Beta-distributed GLMMs only allow the response variable to take on values in the open interval]0;1[, and therefore, all ground cover values were divided by 100. Ground covers were subsequently transformed with a 'lemon-squeezer' transformation (Smithson & Verkuilen, 2006) which concentrates proportional values into the]0;1[interval and draws extreme values away from the interval limits. A

stepwise model reduction was done for each of the 13 GLMMs. Here, global models including the three covariates '*Snow regime'*, '*Vegetation type'* and '*Year',* as well as all 2- and 3-way interactions were reduced to the simplest models possible while keeping the additive terms *'Snow regime'*, *'Year' and 'Vegetation type'* fixed. This was done by sequentially removing one term from the model and comparing model Chi-squares at each step between current (reduced) and previous (more complex) model. Model reduction was stopped if $p < 0.05$ for the Chi-squares test. Model residuals were examined at each step through the 'DHARMa' R-package (Hartig, 2021), applying visual inspection of residual plots as well as several tests for goodness-of-fit. Model structures of the 13 final models are presented in Table 6. All models included a nested random term to account for the spatial variability between fence locations as well as the inherent between-plot differences in *Dryas* and *Cassiope* cover described by the variable *'DES'*. This random term reflected the nested nature of the experimental design. For some models, it was necessary to allow variance to differ between fence locations, snow regimes, DES, or combinations of these, in order to get an acceptable model-fit (as judged from residual diagnostics in DHARMa). Predictor variables which were contributing to significant within-group deviations from residual uniformity in those models were identified by plotting scaled residuals against each predictor variable separately. Variance was then allowed to differ between levels of the identified predictors by applying the 'dispformula'-option in 'glmmTMB' to the affected global models. Model selection was then repeated for those models. The applied dispersion formulas are also given in Table 6.

2.5.3 Effect of snow regime, vegetation type, and year on vegetation indices

The effects of snow regime, vegetation type, and year on VIs was analysed for the following RGB-based indices: Green Chromatic Coordinate (GCC), Greenness Index (GI), Excess Green (ExG) and 2G_RBi, as well as for NDVI obtained with two different sensors: non-imaging GreenSeeker NDVI sensor and MAPIR 3 RGN camera (from here referred to as 'GS-NDVI' and 'MAPIR-NDVI'). The four RGB-based VIs were selected from a list of six candidate VIs since these had the best correlations with MAPIR-NDVI in 2021 according to linear regressions. This was done as it was of interest to investigate if RGB-based VIs could be used for vegetation monitoring in place of the widely used NDVI. Therefore, RGB indices which reflected the properties of NDVI were chosen for this analysis. The correlation between

GS-NDVI and MAPIR-NDVI was also tested. Adjusted R^2 values for the seven linear regression models are presented in Table 5.

Table 5 Adjusted R^2 values for linear regressions of the following vegetation indices with MAPIR-NDVI in 2021: Green Chromatic Coordinate (GCC), 2G_RBI, Greenness Index (GI), Excess Green (ExG), Excess Green-Red (ExGR), Green-Red Vegetation Index (GRVI), and non-image based GreenSeeker NDVI (GS-NDVI). MAPIR-NDVI was obtained with a MAPIR 3 RGN camera.

Vegetation index	**Correlation with MAPIR-NDVI (adjusted R^2)**
GCC	0.96
2G_RBi	1.00
GI	0.97
ExG	0.96
ExGR	0.77
GRVI	0.23
GS-NDVI	0.39

The relationship between each VI and snow regime (*Ambient* or *Deep*), vegetation type (*Heath* or *Meadow*), and year (2015, 2020, and 2021) was analysed using Linear Mixed-effect Models (LMMs). MAPIR-NDVI was only available for 2021, and therefore the model for this index did not include a term to describe year-to-year variation. All models included a nested random term, same as described for ground cover models (section 2.5.2), to account for spatial variability as well as inherent differences in *Dryas* and *Cassiope* cover between plots. All LMMs were done using the 'glmmTMB'-package in R (Brooks et al., 2017). Similar to the ground cover models described in section 2.5.3, a stepwise model reduction was done for each of the six LMMs. For each VI, a global model including '*Snow regime*, '*Vegetation type* and '*Year'* as well as all 2- and 3-way interactions was reduced to the simplest model possible while keeping the additive terms '*Snow regime'*, '*Vegetation type* and '*Year'* fixed. The global model for MAPIR-NDVI did not include the term '*Year*' and therefore this model did not include a 3-way interaction. The procedure applied was the same as described for the ground cover models, where 'DHARMa' residual diagnostics and Chi-square tests were inquired at each step until the model could be reduced no further. Model structures of the resulting six LMMs are presented in Table 8.

2.5.4 Relationship between vegetation indices and plant cover

Relationships between three VIs (GCC, GS-NDVI and MAPIR-NDVI) and ground cover of 13 ground cover categories were investigated. Due to the extensive nature of this analysis, relationships with plant cover could not be analysed for all VIs. Green Chromatic Coordinate

(GCC) was chosen since it was considered one of the most widely used RGB-based VIs in the Arctic (Anderson et al., 2016, 2017; Parmentier et al., 2021; Westergaard-Nielsen et al., 2013, 2017). The two measures of NDVI (image based MAPIR- and non-image based GS-NDVI) were included in order to compare the performance of an RGB-based VI and the more widely used NDVI when used to describe plant community composition. Further, the two NDVI measures represent a passive (MAPIR) and an active (GS) sensor. Since the two sensors are fundamentally different, it was of interest to test whether they performed differently too, and to see if one was more sensitive to vegetation composition than the other.

To test whether the relationships between the chosen VIs and plant cover differed between snow regimes, vegetation types, and years, analysis of variance (ANOVA) tests were applied. Separate tests were performed for each ground cover category and VI (resulting in 39 tests). Here, VIs were used as response variables. Explanatory variables were, in addition to cover of one specific ground cover category, the additive effects of '*Snow regime'*, '*Vegetation type'*, and '*Year'* as well as their interactions with the ground cover category, according to the model:

$$VI_i \sim Cover\ category_j \times (Snow\ regime + Vegetation\ type + Year) \quad (Model\ 1)$$

where *i* was the i^{th} of the three VIs (GCC, GS-NDVI, and MAPIR-NDVI) and *j* was the j^{th} of the 13 ground cover categories. *'Snow regime'* included two levels (*Ambient* and *Deep*), *'Vegetation type'* also included two levels (Heath and Meadow) and *'Year'* included three levels (2015, 2020, and 2021). Interactions were of specific interest in this analysis as the presence of significant interactions would mean that the relationship between ground cover categories and VIs would differ between snow regimes, vegetation types, or years. It was of interest to reveal any such inconsistencies if present, as these would represent a challenge in the use of VIs for describing and monitoring plant community composition.

3 Results

3.1 Plant community composition

In the dbRDA, the model which best described plant community composition was, according to AIC (in fact an AIC-like criterion based on Chi-squares, described in 2.5.1) and adjusted R^2, the model:

$$[species\ X\ cover] \sim Snow\ Regime + Year + cond\ (Fence\ \times\ DES) \qquad (Model\ 2)$$

where variance described by conditioning (*cond*) variables '*Fence'* (fence location) and '*DES'* and their interaction was partialled out. The [species X cover] matrix included per cent ground cover of the plants described in section 2.3.1 and Table 3 (left column). '*Snow regime'* included two levels (*Deep* and *Ambient*) while '*Year*' included three levels (2015, 2020, and 2021). AIC and adjusted R^2 values are given for all candidate models in Table S1.

Vegetation type did not describe any significant amount of variance in plant community composition according to the conducted permutation tests ($p > 0.05$; 999 permutations). The term *'Vegetation type'* and its interaction with *'Snow regime'* were therefore excluded from the final model (Model 2). Addition of the interaction term *'Snow regime × Year'* did not improve the model fit ($\Delta AIC = 1.3$, $\Delta adj\text{-}R^2 = -0.012$) and thus, no interaction was found between snow regime and year. The model accounted for 43.8% of the total variance in community composition. Of this, 13.7% was explained by the variables *'Snow regime'* and *'Year'* while 30.1% was explained by the conditioning variables '*Fence'* and '*DES'*. After removing the contribution of the conditioning variables, snow regime accounted for 14.2% of the variance in community composition ($F = 33.1$, $p < 0.001$). Year accounted for 3.0% ($F = 3.89$, $p < 0.001$) after snow regime had already been accounted for. Plant communities in *Deep* and *Ambient* snow regimes clearly separated in ordination space (Figure 6). Snow regimes separated primarily along the first constrained axis (CAP1) which explained 15.2% of community variance. Here, *Ambient* plots generally had negative loadings while *Deep* plots had positive loadings (Figure 6.B). The three years separated clearly along the second constrained axis (CAP2) which explained 3.0% of community variance. Here, 2015 had a highly negative loading while 2021 had a highly positive loading on CAP2. Even though CAP2 only captured a small amount of community variance the effect of year was still significant according to permutation tests. Live material of the shrubs *Dryas*,

Figure 6. Distance-based redundancy analysis (dbRDA) of the effect of 'Snow Regime' (Deep or Ambient) and 'Year' (2015, 2020 or 2021) on plant community composition in permanent vegetation plots in Adventdalen, Svalbard. The axes shown are the first and second axes of the constrained ordination (CAP1 and CAP2, respectively) given by model 2. These two axes explain a total of 18.2% of plant community variance between plots. A: Plots in Ambient (green) and Deep snow (orange) and ellipses showing 95% confidence intervals for the years 2015, 2020 and 2021. B: Centroids of Snow regimes (Ambient and Deep) and Years (2015, 2020 and 2021) as well as loadings of plant species in the CAP1/CAP2 ordination space. Only plants with positive or negative loadings greater than 0.4 on either axis are shown. Dryas(D) and Cassiope(D) refer to dead plant material while regular plant names refer to live material. Thirty-nine (39) plots were included in 2015 while 123 plots were included in 2020-2021. Note: different axis scales between subplots.

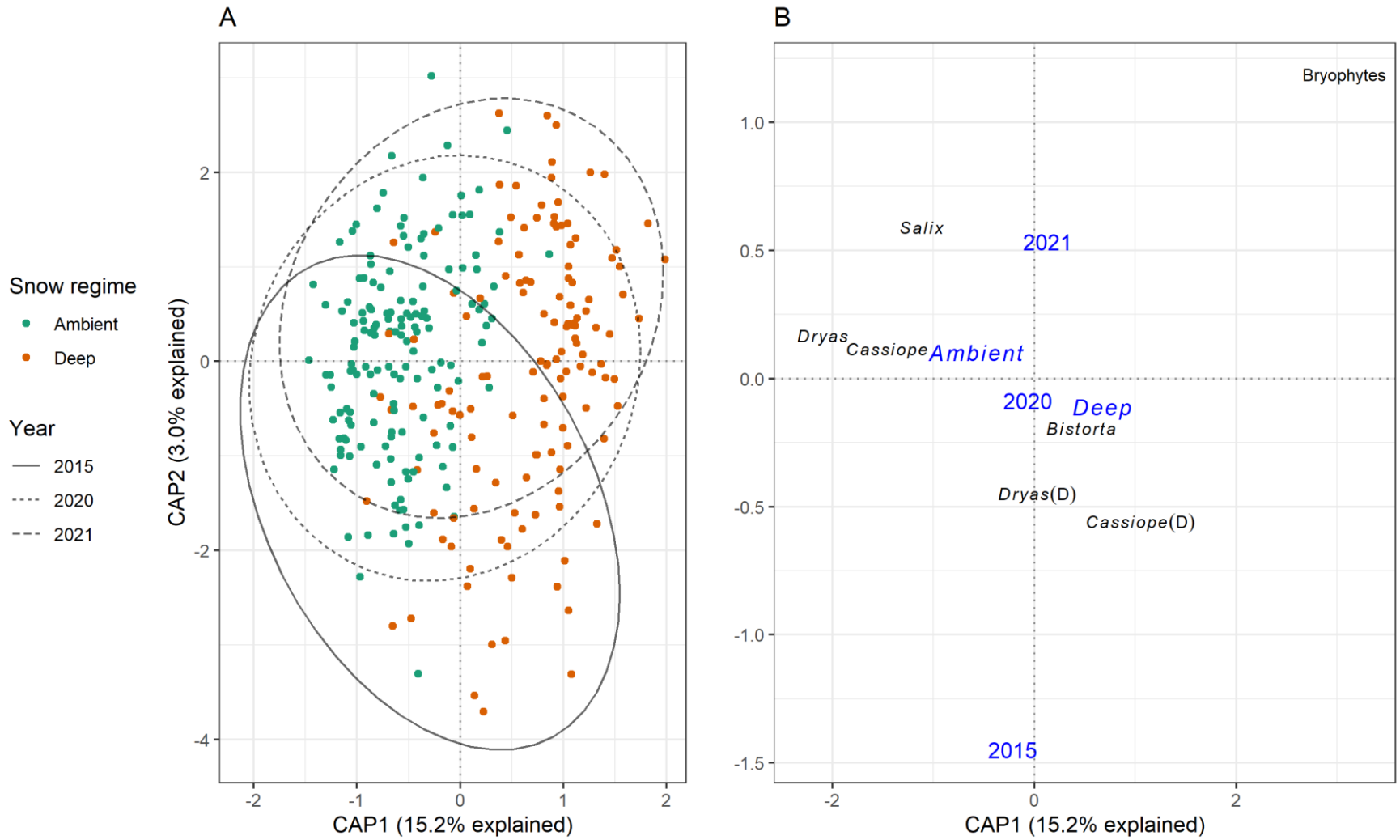

Cassiope, and *Salix* had clear negative loadings on the CAP1 axis. Especially live *Dryas* and *Cassiope* clustered in association with *Ambient* plots while live *Salix* appeared to associate with both *Ambient* plots and the year 2021. Live *Bistorta* and dead *Cassiope* had positive loadings on the CAP1 axis, and clustered in association with *Deep* plots. Bryophytes had highly positive loadings on both the CAP1 axis and the second constrained axis (CAP2).

3.2 Cover of individual plant species and functional groups

The additive effect of snow regime significantly influenced all ground cover categories except live graminoids (Figure 7; Table 7). Here, all p-values were below 0.001 with exceptions only in the two categories 'Lichens' and 'Soil & biocrust'. *Deep* snow had a negative impact on the cover of all categories which contained live plants, except live *Bistorta* and bryophytes where the effect of *Deep* snow was instead positive. *Deep* snow positively affected the cover of dead vascular plants and dead shrubs as well as soil & biocrust with the estimates for dead vascular plants and dead shrubs being highly significant ($p < 0.001$). Dead vascular plant cover decreased between 2015-2021 while bryophytes and live *Salix* both increased between 2015-2021.

The additive effect of vegetation type (Heath or Meadow) impacted the cover of dead and live shrubs, live graminoids, live *Dryas* and live *Bistorta* (Figure 7; Table 7). Here, Heath contained more dead and live shrubs, especially live *Dryas*, than Meadow. Meadow contained more live graminoids and live *Bistorta*. *Deep* snow generally had a stronger effect in Heath than in Meadow, with a more pronounced negative impact on total live plants, live shrubs, and live *Dryas*, as indicated by the significant interactions between snow regime and vegetation type in these plant categories (Table 7). The positive responses to *Deep* snow in dead vascular plants and dead shrubs were also greatest in Heath compared to Meadow. Bryophytes showed a different pattern, with the positive effect of *Deep* snow being more pronounced in Meadow. Live graminoid cover decreased under *Deep* snow in Meadow only. Year-to-year variation further differed between Heath and Meadow in total live plants, live vascular plants, live graminoids and lichens. Although the interaction '*Vegetation type* × *Year'* was significant for these categories, it should be noted that the categories showed significance ($p < 0.05$) only in one or none of the additive terms included in this interaction. Total live plant cover increased between 2015-2021 but only in Heath. Live vascular plant cover was similar in Heath and Meadow in 2015 but smaller in Meadow compared to Heath

in 2020-2021. Live graminoid cover in Meadow was about two times greater in 2015 compared to 2020-2021. Lichen cover was greatest in 2020 but this was due to an increase in Heath only. For dead vascular plants, the positive effect of *Deep* snow decreased between 2015-2021 in Heath while remaining similar among years in Meadow (Figure 7), as indicated by the significant three-way interaction *'Vegetation type × Snow regime × Year'* (Table 7).

Table 6. Included model terms in best candidate models (GLMMs) resulting from the model selection for 13 ground cover categories (responses). Cover groups 'Cassiope', 'Dryas', Salix, and 'Bistorta' refer to live plant material only. All ground covers were modelled with a beta distribution and logit link function. Each model included an identical random factor where 'Dominant Evergreen Shrub (DES)' was nested within snow fence location, in addition to the model terms shown. Some models included an additional dispersion formula. In these cases, the dispersion formulas are shown.

	Model terms							
Response	*Vegetation type*	*Year*	*Snow regime*	*Vegetation type × Snow regime*	*Vegetation type × Year*	*Year × Snow regime*	*Vegetation type × Year × Snow regime*	Dispersion formula
Total live plants	X	X	X	X	X	-	-	-
Live vascular plants	X	X	X	-	X	-	-	-
Dead vascular plants	X	X	X	X	X	X	X	-
Live shrubs	X	X	X	X	-	-	-	-
Dead shrubs	X	X	X	X	-	-	-	-
Live graminoids	X	X	X	X	X	-	-	*~Fence*
Bryophytes	X	X	X	X	-	-	-	-
Lichens	X	X	X	-	X	-	-	-
Soil & biocrust	X	X	X	-	-	-	-	*~Fence × DES*
Cassiope	X	X	X	-	-	-	-	*~Snow regime × DES*
Dryas	X	X	X	X	-	-	-	*~ Snow regime × DES*
Salix	X	X	X	-	-	-	-	-
Bistorta	X	X	X	-	-	-	-	*~Fence*

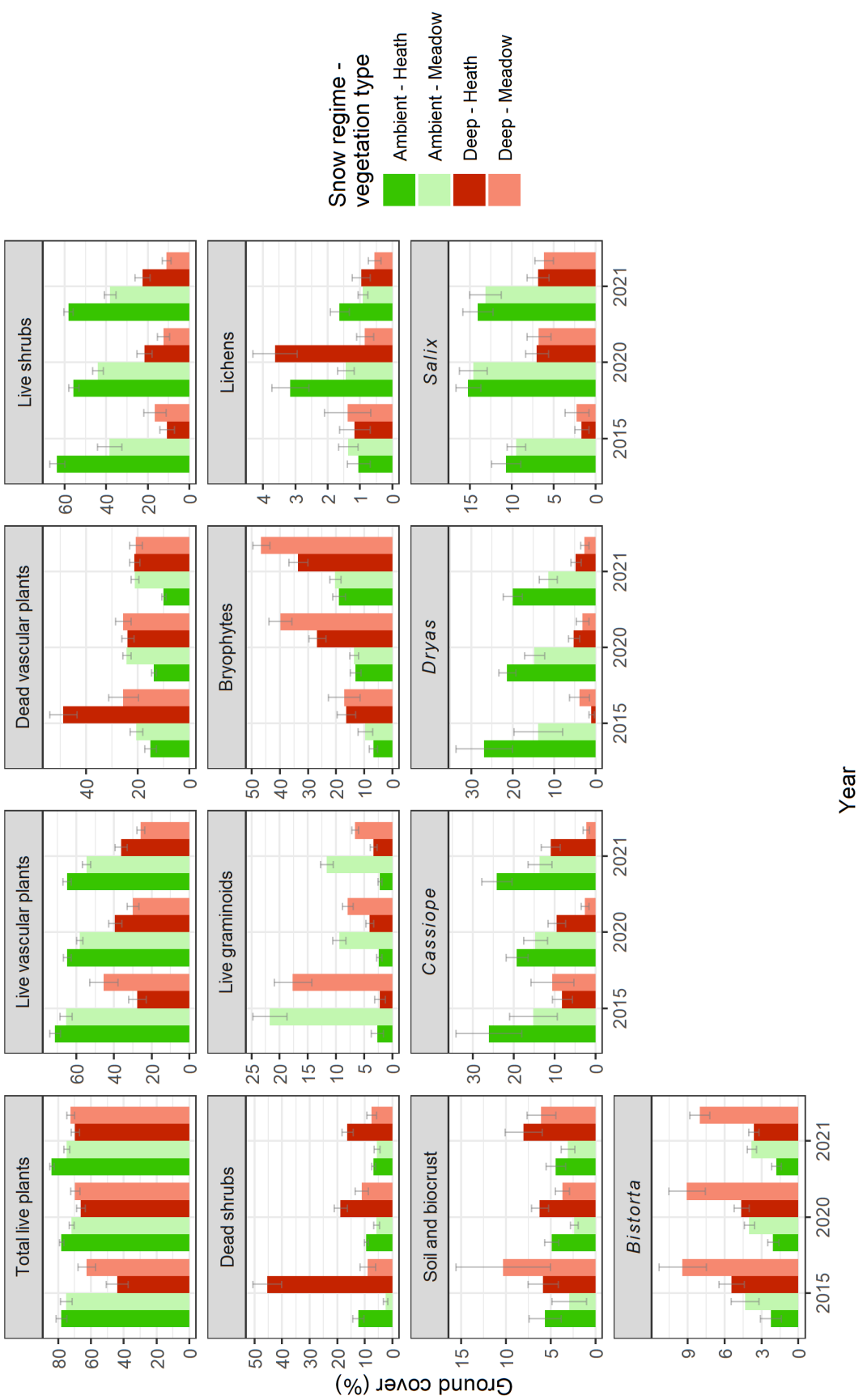

Figure 7. Mean per cent ground cover of 13 ground cover categories in Adventdalen, Svalbard, in years 2015, 2020 and 2021. Covers are shown separately for the snow regimes 'Ambient' (green colours) and 'Deep' (red colours), and for the vegetation types 'Heath' (strong colours) and 'Meadow' (light colours). Error bars indicate standard errors. Note different axis scales for ground cover.

Table 7. Slope estimates ± standard errors for model terms in 13 GLMMs, each modelling per cent ground cover of an individual ground cover category as response, using the model terms 'Vegetation type' (Heath/Meadow), 'Snow regime' (Ambient/Deep) and 'Year' (2015/2020/2021) and interactions when relevant. 'Cassiope', 'Dryas', 'Salix', and 'Bistorta' refer to live material only All values are presented on the logit-scale. Empty fields indicate that the model term was not included in the model for that specific ground cover category. See Table 6 for details on model structures. Significant terms are highlighted in bold, and significance levels indicated with asterisks ('': p < 0.05, '**': p < 0.01, '***': p < 0.001). Significance levels for model intercepts are not shown.*

Model Term	Ground cover category (response)												
	Total live plants	**Live vascular plants**	**Dead vascular plants**	**Live shrubs**	**Dead shrubs**	**Live graminoids**	**Bryophytes**	**Lichens**	**Soil & biocrust**	***Cassiope***	***Dryas***	***Salix***	***Bistorta***
Intercept	1.28 ± 0.23	0.90 ± 0.23	-1.39 ± 0.28	0.96 ± 0.24	-0.83 ± 0.28	-2.85 ± 0.30	-2.36 ± 0.25	-2.26 ± 0.27	-2.17 ± 0.30	-0.7 ± 0.45	-0.63 ± 0.34	-1.47 ± 0.19	-2.85 ± 0.21
Snow regime													
Ambient → *Deep*	**-2.00 ± 0.24** ***	**-1.67 ± 0.1** ***	**2.72 ± 0.36** ***	**-2.33 ± 0.15** ***	**1.13 ± 0.13** ***	0.10 ± 0.27	**0.83 ± 0.14** ***	**-0.25 ± 0.12** *	**0.22 ± 0.11** *	**-1.33 ± 0.15** ***	**-2.06 ± 0.19** ***	**-1.14 ± 0.11** ***	**0.77 ± 0.1** ***
Year													
2015 → 2020	0.00 ± 0.23	0.17 ± 0.20	0.07 ± 0.29	0.05 ± 0.15	**-1.09 ± 0.17** ***	0.02 ± 0.26	**0.79 ± 0.17** ***	**0.86 ± 0.25** ***	0.06 ± 0.17	-0.25 ± 0.16	-0.04 ± 0.16	**0.53 ± 0.17** **	-0.12 ± 0.13
2015 → 2021	0.41 ± 0.23	0.07 ± 0.19	-0.35 ± 0.29	0.03 ± 0.15	**-1.39 ± 0.17** ***	0.29 ± 0.26	**1.23 ± 0.17** ***	0.01 ± 0.26	0.17 ± 0.17	-0.14 ± 0.16	-0.22 ± 0.16	**0.5 ± 0.17** **	-0.18 ± 0.13
Vegetation type													
Heath → Meadow	-0.03 ± 0.29	0.21 ± 0.33	0.51 ± 0.38	**-0.94 ± 0.28** ***	**-1.77 ± 0.41** ***	**3.23 ± 0.35** ***	0.09 ± 0.26	0.08 ± 0.36	-0.41 ± 0.35	-0.72 ± 0.57	**-0.85 ± 0.42** *	0.03 ± 0.16	**0.9 ± 0.24** ***
Snow regime × Vegetation type													
Ambient/Heath → *Deep*/Meadow	**0.96 ± 0.17** ***		**-2.52 ± 0.49** ***	**0.66 ± 0.21** **	**-0.65 ± 0.19** ***	**-0.54 ± 0.19** **	**0.66 ± 0.2** ***				**0.59 ± 0.22** **		
Year × Vegatation type													
2015/Heath → 2020/Meadow	-0.50 ± 0.26	**-0.79 ± 0.29** **	0.24 ± 0.39			**-1.67 ± 0.27** ***		**-0.99 ± 0.36** **					
2015/Heath → 2021/Meadow	**-0.65 ± 0.26** *	**-0.87 ± 0.29** **	0.43 ± 0.39			**-1.62 ± 0.27** ***		**-0.32 ± 0.36**					
Snow Regime × Year													
Ambient/2015 → *Deep*/2020			**-2.00 ± 0.41** ***										
Ambient/2015 → *Deep*/2021			**-1.82 ± 0.42** ***										
Snow regime × Vegetation type × Year													
Ambient/Heath/2015 → *Deep*/Meadow/2020			**1.67 ± 0.56** **										
Ambient/Heath/2015 → *Deep*/Meadow/2021			**1.47 ± 0.56** **										

3.3 Vegetation indices

Clear differences between *Ambient* and *Deep* snow regimes were found in all six VIs (Figure 8; Table 9) with a uniform response in all indices showing lower values in *Deep* snow compared to *Ambient*. All indices showed high significance for the term *'Snow regime'* ($p < 0.001$).

Vegetation index values varied between years in all indices (except MAPIR-NDVI where the model did not include the term *'Year'*). In ExG, GI and GCC, values were lowest in 2015, and increased to similar levels between 2020-2021. The index 2G_RBi also showed lowest values in 2015 but was greater 2020 than in 2021. GS-NDVI was highest in 2020 and lowest in 2021 with the 2015 mean falling between those years. The negative effect of snow regime was similar among years in all indices (Figure 8; Table 9).

The additive effect of vegetation type on VIs was only significant for MAPIR-NDVI with Meadow being higher than Heath ($p < 0.001$; Table 9). However, all four RGB-based VIs (ExG, GI, GCC, and 2G_RBi) showed a stronger negative response to *Deep* snow in Heath than in Meadow (significant interaction *'Snow regime × Vegetation type'*; Table 9).

Table 8. Included model terms in best candidate models (LMMs) resulting from the model selection for 6 vegetation indices, including four RGB (Red-Green-Blue) indices and NDVI measured with two different sensors (non-imaging, active GreenSeeker and imaging, passive 'MAPIR'). All vegetation indices were modelled with a gaussian distribution. Each model included an identical random factor where 'Dominant Evergreen Shrub (DES)' was nested within snow fence location, in addition to the model terms shown. 'MAPIR-NDVI' was only measured in one year (2021) and thus did not include the term 'Year'.

	Model term						
Vegetation Index (response)	*Vegetation type*	*Year*	*Snow regime*	*Snow regime × vegetation type*	*Year × Vegetation type*	*Snow regime × year*	*Vegetation type × Year × Snow regime*
ExG	X	X	X	X	-	X	-
2G_RBi	X	X	X	X	-	X	-
GI	X	X	X	X	-	X	-
GCC	X	X	X	X	-	X	-
GreenSeeker-NDVI	X	X	X	X	X	-	-
MAPIR-NDVI	X	-	X	-	-	-	-

Table 9. Slope estimates ± standard errors for model terms in 6 LMMs, each modelling different vegetation indices (responses) with the model terms 'Vegetation type' (Heath/Meadow), 'Snow regime' (Ambient/Deep) and 'Year' (2015/2020/2021) and interactions when relevant. Empty fields indicate that the model term was not included in the model for that specific vegetation index. See Table 8 for details on model structures and Table 3 for index equations. Significant terms are highlighted in bold, and significance levels indicated with asterisks ('': p < 0.05, '**': p < 0.01, '***': p < 0.001). Significance levels for model intercepts are not shown.*

	Vegetation index (response)					
Model term	**ExG**	**2G_RBi**	**GI**	**GCC**	**GreenSeeker - NDVI**	**MAPIR-NDVI**
Intercept	0.03 ± 0.01	6.4 ± 2.48	0.02 ± 0.01	0.34 ± 0.00	0.47 ± 0.02	0.36 ± 0.01
Snow regime						
Ambient → *Deep*	**-0.05 ± 0.01 *****	**-10.31 ± 2.76 *****	**-0.04 ± 0.01 *****	**-0.02 ± 0.00 *****	**-0.1 ± 0.01 *****	**-0.04 ± 0.01 *****
Year						
2015 → 2020	**0.10 ± 0.01 *****	**19.76 ± 2.07 *****	**0.06 ± 0.01 *****	**0.03 ± 0.00 *****	**0.06 ± 0.02 ****	
2015 → 2021	**0.07 ± 0.01 *****	**16.24 ± 2.03 *****	**0.05 ± 0.01 *****	**0.02 ± 0.00 *****	**-0.05 ± 0.02 ***	
Vegetation type						
Heath → Meadow	0.01 ± 0.01	-1.14 ± 2.54	0.00 ± 0.01	0.00 ± 0.00	0.03 ± 0.03	**0.02 ± 0.01 ****
Snow regime X vegetation type						
Ambient/Heath → *Deep*/Meadow	**0.02 ± 0.01 ***	**6.06 ± 2.00 ****	**0.02 ± 0.01 ***	**0.01 ± 0.00 ***		
Year X vegetation type						
2015/Heath → 2020/Meadow					-0.04 ± 0.03	
2015/Heath → 2021/Meadow					0.03 ± 0.03	
Snow regime X year						
Ambient/2015 → *Deep*/2020	-0.01 ± 0.02	-1.99 ± 3.01	0 ± 0.01	0 ± 0.01		
Ambient/2015 → *Deep*/2021	0.01 ± 0.02	2.7 ± 2.95	0.01 ± 0.01	0 ± 0.01		

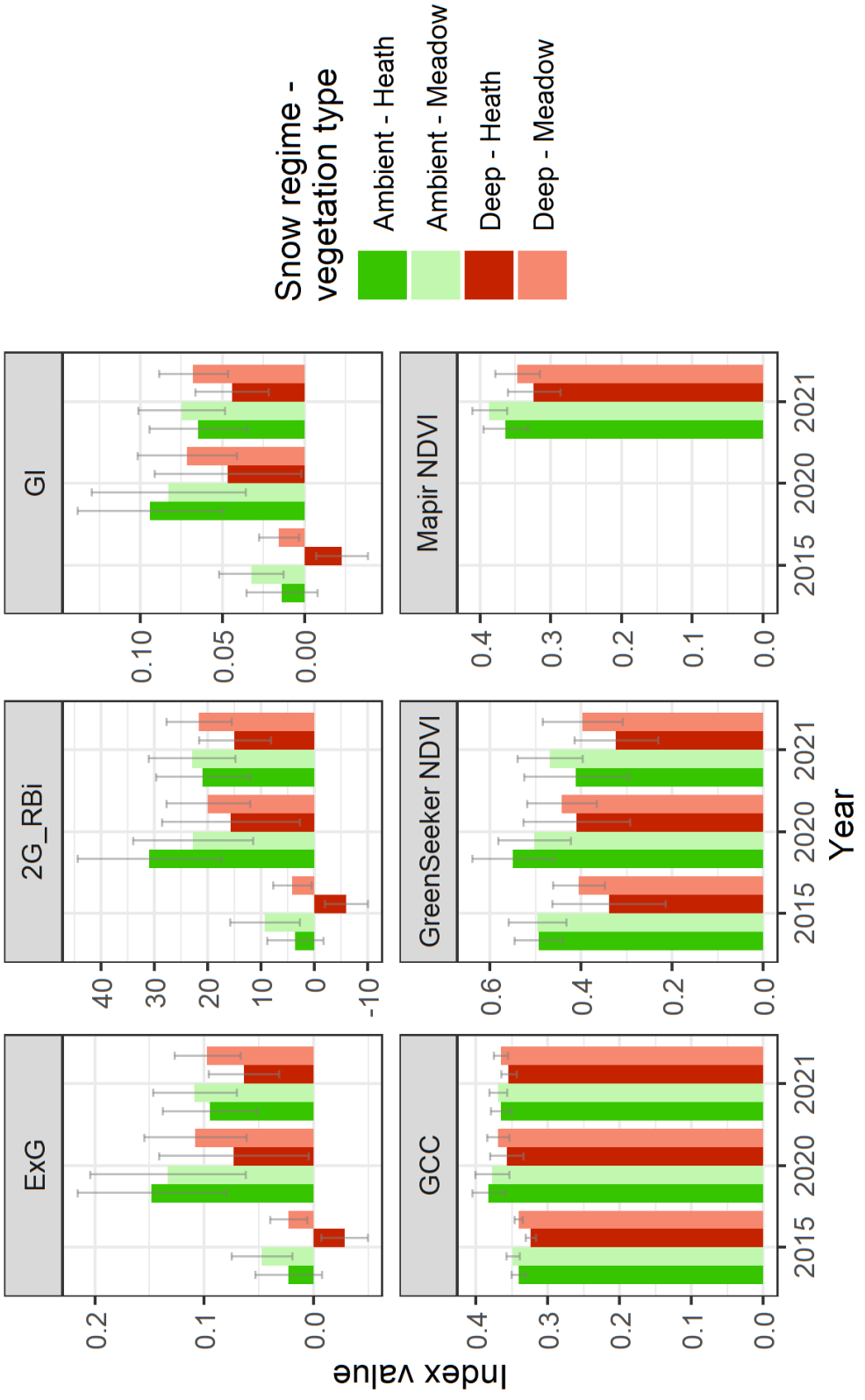

Figure 8. Mean values of 6 vegetation indices of permanent plots in years 2015, 2020 and 2021 in Adventdalen, Svalbard. Covers are shown separately for the snow regimes 'Ambient' (green colours) and 'Deep' (red colours), and for the vegetation types 'Heath' (strong colours) and 'Meadow' (light colours). Error bars indicate standard errors.

3.4 GCC and NDVI relationships with plant cover

Most ground cover categories showed significant correlations with VIs (GCC, GS-NDVI and MAPIR-NDVI; Table 10). Live *Bistorta* did not show significant correlations with GCC, nor did bryophytes in Heath. Lichen cover did not show significant correlations with any of the three VIs.

Linear relationships between plant cover and VIs (GCC, GS-NDVI and MAPIR-NDVI) generally remained similar in slope direction for all VIs across snow regimes, years, and vegetation types. However, slope direction sometimes varied between vegetation types or snow regimes for live vascular plants and live *Cassiope* (Figure 9-11). In most plant groups, the magnitude (i.e., slope) of responses was not the same between years, nor between vegetation types (Figure 9-11), as indicated by the significant interactions between *'Ground cover category'* and *'Year'* and/or *'Vegetation type'* (Table 10). Green Chromatic Coordinate showed different response magnitudes between Heath and Meadow for 8 out of 13 ground cover categories. Furthermore, response magnitudes varied between snow regimes for the plant categories live *Dryas*, live *Cassiope*, and dead shrubs. For GS-NDVI, the magnitude of responses varied between Heath and Meadow in 5 out of 13 plant groups but remained similar between years, with exceptions in total live plants, live vascular plants, and dead vascular plants. The relationships between GS-NDVI and plant cover also varied between snow regimes in the categories live *Dryas* and live shrubs. Further, relationships with MAPIR-NDVI were different in *Deep* and *Ambient* snow regimes for total live plants, dead vascular plants, and live *Bistorta*. Plant cover and MAPIR-NDVI showed the same relationship between Heath and Meadow in ground cover categories.

Table 10. Summary of 13 ANOVA-tests done for each of the three vegetation indices; Green Chromatic Coordinate (GCC), GreenSeeker-NDVI and MAPIR-NDVI as responses. Each test included one 'Ground cover category' and its interactions with Year (2015, 2020, 2021), Snow regime (Ambient/Deep) and Vegetation type (Heath/Meadow). The categories 'Cassiope', 'Dryas, 'Salix', and 'Bistorta' refer to live plant material only. MAPIR-NDVI was only recorded in 2021 and thus 'Year' was excluded from the tests done for this index. All additive effects were included in the tests but only 'Ground cover category' is shown in this table. Significant terms (p < 0.05) are marked with 'X' while non-significant terms are marked with '-'.

	GCC				**GreenSeeker NDVI**				**MAPIR NDVI**		
Ground cover category	*Category*	*Category × Year*	*Category × Snow regime*	*Category × Veg. type*	*Category*	*Category × Year*	*Category × Snow regime*	*Category × Veg. type*	*Category*	*Category × Snow regime*	*Category × Veg. type*
Live plants	**X**	**X**	-	**X**	**X**	**X**	-	-	**X**	**X**	-
Dead plants	**X**	**X**	-	**X**	**X**	-	-	-	**X**	**X**	-
Live vascular	**X**	**X**	-	**X**	**X**	**X**	-	**X**	**X**	-	-
Bryophytes	-	-	-	**X**	**X**	**X**	-	**X**	**X**	-	-
Lichens	-	-	-	-	-	-	-	-	-	-	-
Soil & biocrust	**X**	**X**	-	-	**X**	-	-	**X**	**X**	-	-
Live shrubs	**X**	**X**	-	**X**	**X**	-	**X**	**X**	**X**	-	-
Dead shrubs	**X**	**X**	**X**	-	**X**	-	-	-	**X**	-	-
Live graminoids	-	-	-	**X**	-	-	-	-	**X**	-	-
Cassiope	**X**	-	**X**	**X**	-	-	-	-	-	-	-
Dryas	**X**	-	**X**	-	**X**	-	**X**	-	**X**	-	-
Salix	**X**	**X**	-	**X**	**X**	-	-	**X**	**X**	-	-
Bistorta	-	-	-	-	**X**	-	-	-	**X**	**X**	-

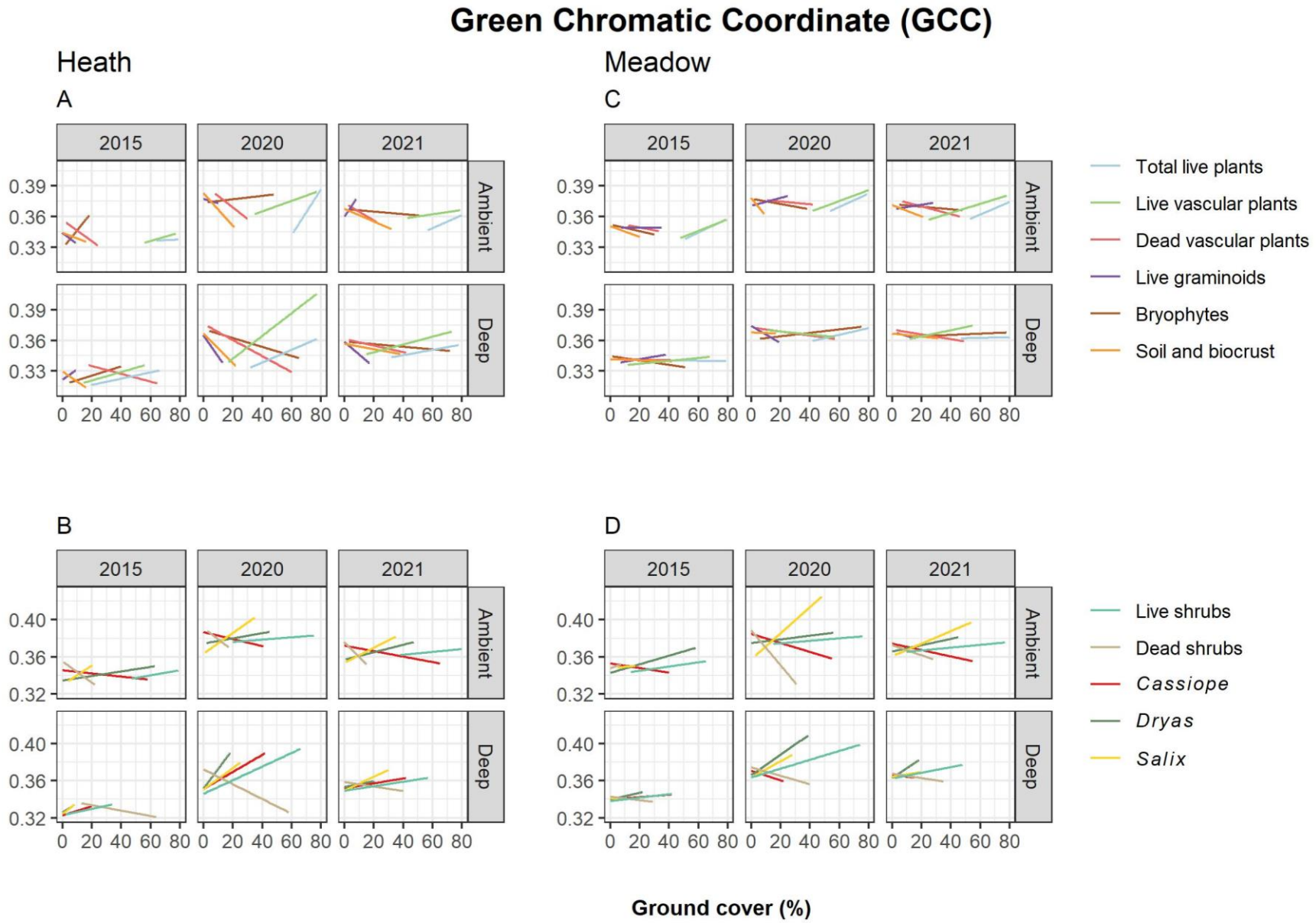

Figure 9. Linear regressions for ground cover categories with Green Chromatic Coordinate (GCC) in three Years (2015, 2020 and 2021) and two Snow regimes (Deep and Ambient) in Heath and Meadow vegetation types, respectively. All shown ground cover categories have significant relationships with GCC according to ANOVA ($p < 0.05$; Table 10). Ground cover categories which did not have significant relationships with GCC are excluded. The categories 'Cassiope', 'Dryas', and 'Salix' refer to live plant material only.

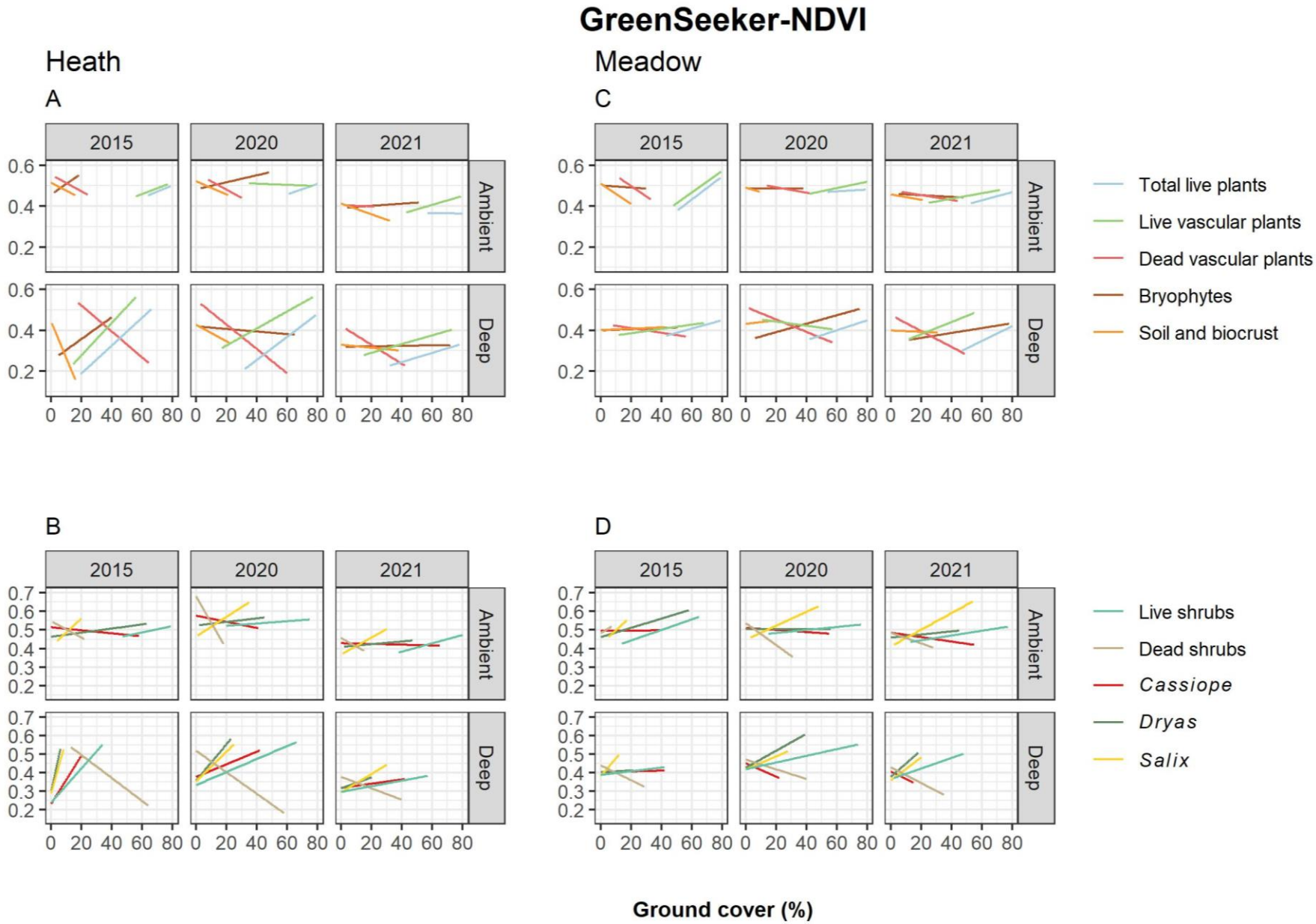

Figure 10. Linear regressions for ground cover categories with GreenSeeker (GS)-NDVI in three Years (2015, 2020 and 2021) and two Snow regmes (Deep and Ambient) in Heath and Meadow vegetation types, respectively. All shown ground cover categories have significant relationships with GreenSeeker according to ANOVA ($p < 0.05$; Table 10). Cover categories which did not have significant relationships with GS-NDVI are excluded. The categories 'Cassiope', 'Dryas', and 'Salix' refer to live plant material only.

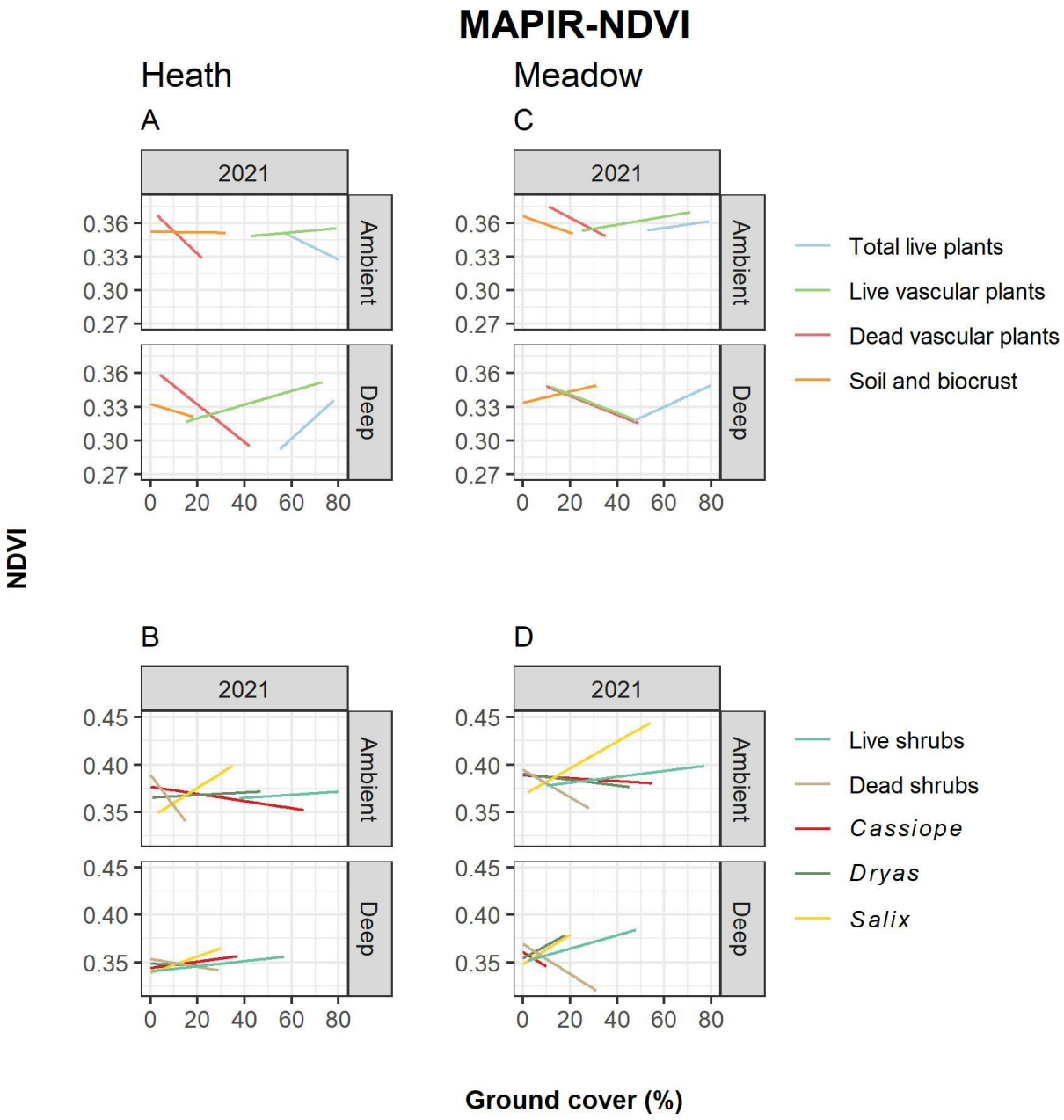

Figure 11. Linear regressions for ground cover categories with MAPIR-NDVI in 2021 and two snow regimes (Deep and Ambient) in Heath and Meadow vegetation types, respectively. All shown ground cover categories have significant relationships with MAPIR-NDVI according to ANOVA ($p < 0.05$; Table 10). Ground over categories which did not have significant relationships with MAPIR-NDVI are excluded. The categories 'Cassiope', 'Dryas', and 'Salix' refer to live plant material only.

4 Discussion

4.1 Summary of results

This study demonstrates clear changes in plant community composition after 15 years of experimentally deepened snow in Adventdalen, Svalbard (Figure 6-7; Table 7). Live cover of the shrubs *Cassiope*, *Dryas*, and *Salix* declined in *Deep* snow while bryophytes increased. *Deep* snow had more dead vascular plant material, and this was especially from dead shrubs in Heath. However, dead shrub cover declined between 2015-2021. The overall effect of deepened snow did not appear to get larger with time but generally remained similar in 2015, 2020 and 2021. Heath and Meadow vegetation types responded to deepened snow in a similar manner, but community changes were more pronounced in Heath.

The RGB-based VIs (ExG, 2G_RBi, GI, and GCC) as well as image based and non-image based NDVI (MAPIR-NDVI and GS-NDVI) all showed similar patterns across snow regimes and years (Figure 8, Table 9). *Deep* plots had lower VI values than *Ambient* plots, possibly reflecting the differences in plant community composition described for the two snow regimes. Vegetation indices generally remained similar between vegetation types but *Deep* snow affected Heath more negatively than Meadow. This is concurrent with the larger community changes also seen in Heath vegetation. Vegetation indices varied among years and were generally lowest in 2015 while differences between 2020 and 2021 were only observed in GS-NDVI.

Relationships between VIs (GCC, GS-NDVI, and MAPIR-NDVI) and cover of individual plant species/functional groups varied in magnitude and sometimes direction between vegetation types, years and/or snow regimes for most plant species and functional groups. However, directions of these relationships were generally similar between years, snow regimes, and vegetation types.

4.2 Plant community

The changes in plant community documented here after 15 years did not show very different trends from the changes documented after 9 years by Cooper et al. (2019) within the same experiment. This indicates that some of the vegetation changes described here likely happened before 2015, and that the effect of deepened snow generally did not get larger with time. Since 2015, total live plant cover has increased in *Deep* snow while dead vascular plant

cover (mostly from dead shrubs) has decreased (Figure 7; Table 7). The latter trend suggests that shrub die-back most likely happened sometime before 2015, due to the installation of the snow fences, and since then, dead plant material has been disappearing from the plots. Distance-based redundancy analysis revealed general differences in community composition between snow regimes and years. The arrangement of the three years on the CAP2 axis (Figure 6) indicates a temporal development in the plant community between 2015-2021 with changes happening independently of snow regimes, especially in *Salix* and bryophytes. This was supported by GLMMs which further documented general decreases in live graminoids in Meadow vegetation (Figure 7, Table 7). However, differences between snow regimes were more pronounced, showing that snow depth is an important driver of plant community change in the study system. The dbRDA did not indicate any significant differences in plant communities between Heath and Meadow vegetation types but this result was contrasted when modelling plant cover for each species separately using GLMMs (Figure 7, Table 7). Here, 10 of the 13 plant categories showed differences in ground cover between vegetation types when interactions were included in the models. The three categories which never differed between Heath and Meadow vegetation types were: live *Cassiope*, live *Salix*, and 'Soil & biocrust'.

A general trend was seen where bryophyte cover showed a steady increase in both snow regimes between 2015-2021. However, the increase was greatest in *Deep* snow, and especially in Meadow where bryophyte cover had increased about three-fold since 2015 (Figure 7). In 2021, bryophyte cover was more than twice as extensive in *Deep* than *Ambient* in the Meadow habitat. Hence, bryophytes was the only plant group which saw significantly larger changes in Meadow than Heath under *Deep* snow (see term *'Snow regime × Vegetation type'*; Table 7). In fact, the opposite trend (i.e., larger changes in Heath) was observed in several plant categories (total live plants, dead vascular plants, dead shrubs, live shrubs, live graminoids and live *Dryas*) where the interaction terms *'Snow regime × Vegetation type'* were significant (Table 7). This is contrasting to the findings of Mörsdorf & Cooper (2021) which concluded that changes were greatest in Meadow when combined with experimental summer warming. These results indicate that Heath vegetation may be more vulnerable to changes under altered snow conditions compared to Meadow vegetation. Anyhow, this study did document a decrease in live vascular plants in Meadow (mostly from live graminoids) between 2015-2021 (Figure 7), but this reflected a general trend which happened in both

Ambient and *Deep* plots. A likely explanation for the decrease in live graminoids could be intensified grazing pressure from a growing Svalbard reindeer (*Rangifer tarandus platyrhynchus*) population in the study area (see www.mosj.no). Fertilisation by addition of reindeer faeces simultaneously across the study site could also be partly responsible for the general increase in live *Salix* in both *Ambient* and *Deep* snow described here (Figure 7; Table 7; see van der Wal & Brooker, 2004), although this explanation is not comprehensive. It is possible that the marked increase in bryophyte cover in Meadow vegetation over the study period may be due to increasing summer rainfall but unfortunately, summer precipitation data was not available for all study years (seklima.met.no) and hence, this relationship could not be explored further. Increasing bryophyte cover may also be an effect of lower competition from the described decrease in vascular plants, as has also been suggested by Mörsdorf & Cooper (2021). Such a negative relationship between bryophytes and vascular plants is well-established in the Arctic (Cornelissen et al., 2001; Elmendorf et al., 2012; Martin et al., 2017), as well as in Norwegian alpine tundra (Klanderud & Totland, 2005), where bryophytes appear to be at a competitive disadvantage to vascular plants. Wahren et al. (2005) found a similar increase in bryophyte cover in highly increased snow depth (deepened by ~3 m) at a moist tussock tundra site in Toolik Lake, Alaska, USA. This was combined with a decrease in evergreen shrubs but an increase in deciduous shrubs. However, within their study site, bryophytes generally decreased while shrubs increased in most levels of deepened snow. At a dry tundra site, bryophyte cover was found to decrease consistently in all deepened snow regimes while shrubs increased (Wahren et al., 2005). Christiansen et al. (2018) found that evergreen shrubs increased in deepened snow at a mesic tundra site in Daring Lake, Canada. Similarly, for graminoids, contrasting findings have been reported with increases in Abisko, sub-Arctic Sweden (Johansson et al., 2013), and decreases in Toolik Lake (Leffler et al., 2016). This diversity of responses demonstrates that when comparing the effects of deepened snow, one must consider both the level of snow-increase as well as the initial composition of the plant community which is under effect.

Our study site in Adventdalen, Svalbard, is the only site, except Toolik Lake, where increasing bryophyte and decreasing shrub- and graminoid cover has been documented due to a deepened snow regime. This study further documents an increase in the common forb *Bistorta* although this result should be interpreted with some caution as variation in abundance between snow regimes was small. However, Mörsdorf & Cooper (2021) also

documented an increase in *Bistorta* in *Deep* snow when combined with summer warming in our study site using data from 2017, supporting this result. Further, *Bistorta* is often associated with snow-bed communities, and increased forb abundance in *Deep* snow has been observed in several alpine snow manipulation sites (Mark et al., 2015; Wipf & Rixen, 2010). The contrasting findings from this and other studies in the Arctic confirm that community composition responses to climate are highly heterogenous, site-dependent and vegetation type-specific (Bjorkman et al., 2018; Elmendorf et al., 2012; Niittynen et al., 2020; Rixen et al., 2022). It is clear that any response is dependent on the initial state of the plant community (Epstein et al., 2000; Mörsdorf & Cooper, 2021; Wipf & Rixen, 2010) as well as the level of snow increase (Rixen et al., 2022). In this study, however, responses to deepened snow mainly differed in magnitude but not direction between Heath and Meadow vegetation types, albeit with an exception in live graminoids which decreased under deepened snow only in Meadow. It has been suggested that plant functional groups may mask species-specific responses to snow regimes in shrubs (Saccone et al., 2017) but this does not appear to be the case in our study site as all three shrub species (*Cassiope*, *Dryas*, and *Salix*) showed very similar responses (Figure 7; Table 7).

Several abiotic factors have been identified which play important roles in determining plant community composition responses to climate, including soil moisture (Bjorkman et al., 2018; Elmendorf et al., 2012; Kemppinen et al., 2019) and nutrient availability (Mörsdorf et al., 2019; Semenchuk et al., 2015), both of which are altered in *Deep* snow (Morgner et al., 2010; Schimel et al., 2004). Mörsdorf & Cooper (2021) suggested that increased soil moisture soon after snowmelt may be driving shrub die-back due to waterlogging with associated anoxia. Furthermore, shrub growth and reproduction may be especially negatively impacted by the shortened growing season which result from delayed spring-time snow melt as well as by lower summer soil temperatures in *Deep* plots (Cooper et al., 2011). Shrub and graminoid dieback create space which bryophytes and other snow bed plants, such as anoxia-adapted forbs, i.e., *Bistorta*, can colonise (Crawford et al., 1994), presumably under reduced competition (Wijk, 1986). The elevated nutrient availability under deepened snow can enhance both bryophyte (Sjögersten et al., 2010) and forb growth, especially in *Bistorta* (Mörsdorf et al., 2019). Furthermore, the parasitic fungi *Exobasidium hypogenum* Nannf. is known to increase under deepened snow (Moriana-Armendariz et al., 2021), and this may have negative impacts on the common shrub *Cassiope* at our study site.

Plant cover data for this study was obtained by visual ground cover estimates. Here, plant cover is assessed in a subjective estimate by the field worker, and data reliability is therefore dependent on the field worker having a certain level of training in this technique. The method is widely used due to its efficiency which enables biologists to survey many plots in a short amount of time. However, the obtained data is not strictly objective, and should therefore be interpreted with some caution. Here, the researcher must assess whether observed differences in cover represent real changes, or if they could be caused by observer-bias, or simply be artefacts of inaccuracy (especially for small percent-wise differences; Vittoz & Guisan, 2007). An alternative method to visual cover estimation is the point intercept-method, which provides a more objective measure of plant cover. However, this method is time-consuming compared to visual estimation, and would not have been feasible in the case of this study which included 127 vegetation plots. Vittoz & Guisan (2007) compared the two methods and argued that visual estimation is the most appropriate method when working in a setting with high replication due to a trade-off between efficiency and data quality. They further showed that estimate accuracy could be improved when observers worked together in pairs, as was generally done in this study. Similar results have been reported from our study site using both visual cover estimates (Cooper et al., 2019) and point intercepts (Mörsdorf & Cooper, 2021), suggesting that the current vegetation change can indeed be reliably observed by visual cover estimates within the study site.

4.3 Vegetation indices

An interesting finding from this study was that most of the tested RGB-based VIs had very good correlations with the imaging MAPIR-NDVI in our plots (Table 5). Thus, indicating that both GCC, 2G_RBi, GI, ExG and ExGR could potentially be used as substitutes for NDVI in the vegetation types investigated in this study (*Cassiope* Heath and mesic meadow) but with ExGR being inferior to the other indices ($R^2 = 0.77$). A similar, good correlation between ExG and NDVI has also been documented in Toolik Lake, Alaska (Beamish et al., 2016; note ExG is referred to as 'GEI' here), underlining the potential usefulness of ExG as a monitoring tool in Arctic tundra. Of the tested RGB-based VIs, only GRVI had a poor correlation with NDVI ($R^2 = 0.23$) even though GRVI has previously showed strong correlations with GS-NDVI in a phenology study in Advendalen, Svalbard (Anderson et al., 2016, 2017). An inspection of the equations given in Table 3 reveals that 2G_RBi, GI and ExG are calculated from rather similar equations, where GI and ExG are in fact normalised measures of 2G_RBi,

calculated in two different ways. Because of this relatedness of the VIs, it is not surprising that these show the similar patterns documented in this study. However, it is noteworthy that 2G_RBi, GI and ExG show the same general trends as GCC and NDVI across years and snow regimes (Table 9; Figure 8). GS-NDVI had poor correlation with MAPIR-NDVI (R^2 = 0.39; Table 5) and showed much larger variance than MAPIR-NDVI (evident from greater standard errors; Figure 8). Differences between the two NDVI measures can most likely be ascribed to the less standardised use of the GreenSeeker sensor in the field (not mounted on camera frame at fixed height and angle like the MAPIR camera), as well as the smaller ground area measured by the GreenSeeker (30 x 30 cm) which meant that the GreenSeeker was in fact only recording NDVI for a sub-area of each plot.

All tested VIs showed lower values in *Deep* snow than in *Ambient*, and generally reflected the same pattern in Heath and Meadow vegetation types. GS-NDVI was the only index which showed lower values in 2021 compared to 2015, which was the lowest year in all RGB-based VIs (ExG, 2G_RBi, GI and GCC; Figure 8). However, this same year-to-year pattern was revealed when comparing maximum seasonal NDVI values in the same years from a nearby PhenoCam study (Figure 11; described in Parmentier et al., 2021). This suggests that the observed GS-NDVI values are representative for the study area, and highlights differences between RGB-based VIs and NDVI. Only MAPIR-NDVI was able to detect general differences between vegetation types, with Meadow being higher than Heath (Table 9). This confirms that the conventional NDVI is indeed very useful in near-remote sensing of vegetation as the near-infrared band is highly sensitive to vegetation. Unfortunately, MAPIR-NDVI was only available in 2021 and therefore the performance of this NDVI measure could not be compared over several years. I suggest future studies should include an imaging NDVI sensor to test whether this improves the ability to detect vegetation changes over time compared to non-imaging NDVI sensors (such as the GreenSeeker). MAPIR-NDVI was consistently lower than GS-NDVI in the same plots. Presumably, this represents a calibration issue with the MAPIR images, which should be calibrated according to the incident sun/shade conditions at the time of photographing. In this study, all MAPIR RGN images were calibrated with a standard calibration option in the MCC software, imitating a clear, sunny day. This standard calibration may not be the most appropriate option as most days are cloudy in Adventdalen. For future use of the MAPIR camera, I advise the use of a MAPIR Camera Reflectance Calibration Ground Target Package, a calibration plate which can be

photographed, e.g., on each field day, to calibrate images more accurately to the incident light conditions. However, standardisation was achieved in this study by manually shading each plot while the photograph was taken, such that all photographs were taken in similar light conditions. Therefore, the used MAPIR-NDVI values are deemed reliable.

In this study, RGB-based VIs and NDVI generally revealed the same trends even though year-to-year comparisons could not be made for MAPIR-NDVI, and GS-NDVI differed slightly from the RGB-based VIs between years (Figure 8; Table 9). RGB-based VIs and NDVI rely on different parts of the electromagnetic spectrum to measure variation related to vegetation, although both include a measure of visible red reflectance (Table 4). While RGB-based VIs primarily rely on visible green reflectance, NDVI relies on NIR to measure vegetation (Xue & Su, 2017). These different parts of the electromagnetic spectrum inherently reflect different properties in the objects with which they interact. Here, NIR is known to have high reflectance by chlorophyll (Zarco-Tejada et al., 2012) while visible green reflectance is associated more generally with green vegetation (Xiaoqin et al., 2015). Despite the fundamental differences in RGB-based VIs and NDVI, this study shows that both can yield similar results in vegetation monitoring in the high Arctic, in concordance with current knowledge (Beamish et al., 2018; Tømmervik et al., 2014). It should be noted that the MAPIR camera and the GreenSeeker sensor represent two conceptually different types of sensors i.e., a passive, imaging sensor (MAPIR) and an active, non-imaging sensor (GreenSeeker). While passive sensors measure reflectance of ambient radiation, an active sensor emits radiation and subsequently measures the reflection of this radiation. The fundamentally different physical properties of these sensors may also contribute to the differences in recorded MAPIR- and GS-NDVI. It may be argued that, even though they are both measures of NDVI, MAPIR- and GS-NDVI could be considered separate, distinctly different VIs due to the inherent differences in how the two sensors measure reflectance. Further studies on near-remote sensing of vegetation composition may benefit from the use hyperspectral cameras in place of RGB and NIR based cameras/sensors due to the great number of available spectral bands in hyperspectral images. This wealth of spectral bands may be used to create more advanced VIs which could be more sensitive to community composition and vegetation change. However, hyperspectral cameras are expensive and not as widely available as RGB/RGN cameras and NDVI sensors.

A possible confounding factor in this study is the use of different RGB cameras in each year (even though this is merely what can be expected in any long-term experiment or monitoring programme). In this study, there is no way of separating any effects caused by the different cameras from the effects of the vegetation composition on VIs. Automatic camera settings were used including shutter speed, aperture, and ISO. As VIs are fractions of reflectance, these settings, which inherently differ between images, still should not significantly impact the VI values. However, white-balance may influence RGB-based VIs (Richardson, 2019), and this, unfortunately, could be a potential source of error as automatic white-balance settings were used in image collection, and no white-balance calibration target was used. Even though image data was collected with different cameras and with automatic white-balance, the tested RGB-based VIs still revealed general patterns which were similar between years. Here, *Deep* plots were less green than *Ambient* with the largest negative effect of *Deep* snow on VIs in Heath vegetation. This pattern corresponded with the observation that community changes due to deepened snow were greatest in Heath vegetation, suggesting that the VIs are indeed responding to these changes. This suggests that, despite the use of different cameras, RGB-based VIs can be used to detect differences in vegetation over several years.

However, to what extent the observed differences in VIs should be ascribed directly to real changes in plant community composition should be considered with caution. It has been demonstrated that *Deep* snow affects plant phenology at our study site, including green-up timing (Semenchuk et al., 2016). This is very important to consider when interpreting the lower VI values in *Deep* snow. Presumably, phenology is partly responsible for these differences with *Ambient* vegetation being closer to peak-growth, and thus greener, than *Deep* vegetation at the time of data collection. Indeed, RGB-based VIs have often been used to monitor vegetation phenology in the Arctic, including in Svalbard (Anderson et al., 2016, 2017; Parmentier et al., 2021) and Alaska (Beamish et al., 2016, 2018). Hence, it is expected that phenological differences between snow regimes contributed to the higher VI values in *Ambient* than *Deep* described here. Further, NDVI is known to be confounded by moisture (Engstrom et al., 2008). Bryophyte NDVI is especially affected by moisture (May et al., 2018; Valøen, 2019), with high moisture content leading to increased NDVI due to lower reflection of red wavelengths. There is good reason to suspect that such a relationship exists between moisture and RGB-based VIs too, as these indices also include red wavelengths (see Table 4). Since *Deep* plots are moister than *Ambient* plots at our study site (Morgner et al., 2010),

bryophyte contribution to VI values is expected to be more positive in *Deep* snow than in *Ambient.* However, even though moisture does correlate with NDVI at our study site, moisture alone does not appear to explain the variation in peak-growth season NDVI between snow regimes (unpublished data, Elisabeth Cooper).

Unpublished data from a nearby PhenoCam study in Adventdalen, described in Parmentier et al. (2021) and Anderson et al. (2016, 2017), shows that seasonal maximum NDVI value varies between years in a permanent vegetation plot in *Cassiope* heath near our snow fences (Figure 11). The pattern observed in seasonal maximum NDVI values here (2020 higher than 2015 which is higher than 2021) is confirmed by another long-term seasonal NDVI study in Adventdalen (unpublished data, Stein Rune Karlsen). These year-to-year fluctuations appear to be driven by variations in summer temperature, time of snowmelt and summer precipitation which affect green-up and peak-growth timing. This complicates the interpretation of VIs captured at only one time in the growing season like in this study, and it underlines the importance of accounting for these fluctuations in order to meaningfully interpret VI data when describing vegetation change through several years.

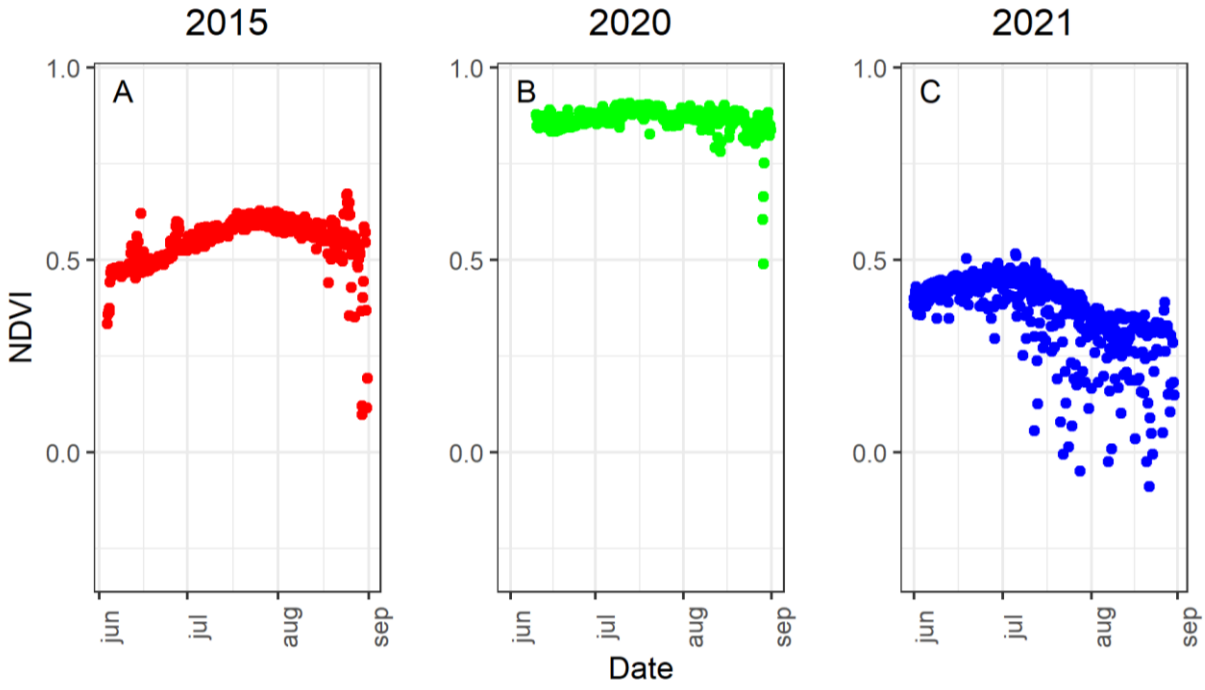

Figure 12. Seasonal NDVI in 2015, 2020 and 2021 at a permanent plot near snow fences A1 and A3 from a phenocam study described in Parmentier et al. (2021). Unpublished data, gathered by Lennart Nilsen.

4.4 Vegetation indices as a monitoring tool for community composition

The inconsistency of responses in VIs, especially GCC, among vegetation types and years to the cover plant species/functional groups presents major challenges in meaningfully using GCC and NDVI as measures of plant community composition over time and space. In this analysis, NDVI performed more consistently than GCC across years. GS-NDVI relationships with plant cover were generally more consistent between study years but still differed in magnitude and sometimes even direction for the major functional groups; total live plants, live vascular plants, and bryophytes (Figure 9-11; Table 10). There was also considerable variation in GS-NDVI responses between Heath and Meadow vegetation types in live vascular plants, live shrubs, live *Salix*, bryophytes, and soil & biocrust. The inconsistent manner in which VIs relate to plant cover over time and space likely renders the use of plot-level GCC or NDVI values quite insufficient for describing ground cover, even for wide functional groups such as total live plants, dead vascular plants, bryophytes, and soil/biocrust. MAPIR-NDVI was the most promising VI measure with no significant variation in response magnitudes between vegetation types in any plant groups, and only between *Deep* and *Ambient* snow regimes in a few plant groups (Figure 11; Table 10). However, the sample size was much smaller for MAPIR-NDVI as it was only collected in 2021, and therefore this result should be interpreted with caution. Additionally, there is no way of testing its performance over several years. I advise that this NDVI measure should be investigated further in future studies

It is hypothesised that the different relationships between VIs and plant cover among years, snow regimes, and possibly also vegetation types, could be partly caused by phenological differences in these at the times of data collection (Semenchuk et al., 2016). Ideally, ground cover estimates and image data collection should take place exactly at the time of peak-growth each year. However, since snowmelt timing, summer temperatures, and precipitation vary between years this can be difficult to achieve in practise due to logistical issues with field work in a remote location. Thus, the collected VI data only provides a snapshot of the plant community structure at a very restricted period of the growing season, which can be highly affected by differences in phenological progression between years.

Graminoid cover has been demonstrated to contribute significantly to NDVI and ExG in Arctic tundra (Beamish et al., 2016; note ExG is referred to as 'GEI' here) but phenological stage will inherently affect VIs as graminoid green-up and growth happens rapidly with large changes over a short time. Beamish et al. (2016) also showed that both evergreen and deciduous shrubs can significantly contribute to NDVI and ExG. In Adventdalen, the very common evergreen shrub *Cassiope* produces dense stands of white flowers (see Figure 5). If VI data is captured at the time of flowering, these white flower stands would be expected to significantly lower plot VI values. This mechanism could perhaps explain the observed pattern where *Cassiope* is positively correlated with GS-NDVI and GCC in *Deep* Heath but negatively in *Ambient* Heath (Figure 9-10). It is known that flowering phenology is delayed in the *Deep* snow regime (Semenchuk et al., 2016) which means that *Cassiope* could potentially be flowering in *Ambient* but not *Deep* at the time of data collection. While this would not influence plant cover estimates it would affect the plot VI values, and thus lead to different relationships between the two in *Ambient* and *Deep* snow regimes. Also, as live *Cassiope* is a rather brown in colour, even in mid-growing season, high *Cassiope* cover would be expected to negatively affect VIs for the categories 'live shrubs' and 'live vascular plants', where the other included plants are greener in mid-summer, especially the shrub *Salix*. This shows that using plant functional groups may not always be appropriate in the study of VIs, as some species-specific responses can be lost. As bryophyte NDVI is affected by moisture (May et al., 2018; Valøen, 2019), it is hypothesised that annual precipitation patterns or fine-scale moisture regimes could perhaps explain the ambiguous relationships between VIs and bryophytes between Heath and Meadow vegetation (Figure 9-11). It has also been noted that bryophyte NDVI signal can sometimes be masked by vascular plants (May & Beamish, 2015). Therefore, the relationship between bryophyte cover and NDVI could potentially vary with vascular plant cover, making interpretation increasingly difficult.

The points discussed here indicate that 'snapshot' measurements of peak-growth season VIs are hardly useful if they are not interpreted in the context of annual variations in maximum VI values (Figure 12) and if phenological stage of the vegetation is not accounted for. This renders near-remotely sensed VIs somewhat easier to interpret in the study of seasonal dynamics rather than year-to-year community changes captured at one time during the year. It remains unresolved how near-remotely sensed VIs can be used to describe changes in vegetation composition in the future. Detailed accounts of phenological stage and maximum

seasonal NDVI may aid interpretation of VIs in this regard. For further studies, hyperspectral cameras will likely provide much greater detail.

4.5 Conclusions

In brief, this study demonstrates clear changes in plant community composition under experimentally deepened snow in Adventdalen, Svalbard, Norway. The changes included decreased shrub- and graminoid cover and simultaneously increased cover of bryophytes and the common forb *Bistorta* in *Deep* snow. Graminoid cover only decreased in Meadow, however, community changes were generally more pronounced in the Heath vegetation, and this was the case in all three study years. This suggests that Heath vegetation may be more vulnerable to changes in snow depth compared to Meadow vegetation. No evidence was found that the effect of deepened snow got larger with time between 2015-2021 as the effect of *Deep* snow was similar in all years for most plant groups. However, dead plant material decreased in *Deep* snow over time which was contrary to expectations. This was ascribed to shrub die-back which happened before 2015, especially in Heath, after which dead plant material has been disappearing from the plots. As a general trend across the study area, bryophytes and *Salix* increased in both *Ambient* and *Deep* snow regimes but bryophyte increase was much greater in *Deep* snow. Live graminoids decreased in both snow regimes, but only in the Meadow vegetation type, and more so in *Deep* than *Ambient*.

To my knowledge, this is the first study to relate vegetation change to near-remotely sensed VIs over several years, let alone to do it in an experimentally deepened snow regime. The tested VIs included four RGB-based VIs (ExG, GI, GCC, and 2G_RBi), as well as the image based MAPIR-NDVI, and the actively sensed, non-image based GS-NDVI. These VIs were able to detect differences between plots in *Ambient* and *Deep* snow regimes, possibly reflecting differences in plant community composition, with smaller VI values in *Deep* plots, especially in the Heath vegetation type. However, the detected differences may, at least in part, relate to phenological progression which also differ between snow regimes. Vegetation index values increased from 2015 to 2020-2021 (which were similar) but these differences could not be directly related to plant community changes. Green Chromatic Coordinate as well as GS- and MAPIR-NDVI correlated with cover of most plant groups, but these relationships differed in magnitude and sometimes even direction between vegetation types, years, and snow regimes. This ambiguity makes it challenging to establish any direct

inference between VIs and ground cover of individual plant species/functional group in this study.

Thus, unresolved challenges remain when it comes to using VIs to make inferences about vegetation change in Arctic tundra. It is thought that annual variations in maximum VI values (likely due to variations in temperature and precipitation) are partly responsible for the unclear relationships described here. I suggest that future studies should investigate the relationship between VIs and plant cover in a context of annual variations in maximum VI values and also include measures of phenological progression. This may render near-remotely sensed VIs useful for monitoring of vegetation change in the future.

Literature cited

Anderson, H. B., Nilsen, L., Tømmervik, H., Karlsen, S. R., Nagai, S., & Cooper, E. J. (2016). Using ordinary digital cameras in place of near-infrared sensors to derive vegetation indices for phenology studies of High Arctic vegetation. *Remote Sensing*, *8*(10). https://doi.org/10.3390/rs8100847

Anderson, H. B., Nilsen, L., Tømmervik, H., Karlsen, S. R., Nagai, S., & Cooper, E. J. (2017). Erratum: Using ordinary digital cameras in place of near-infrared sensors to derive vegetation indices for phenology studies of high arctic vegetation [Remote Sens., 8, (847) (2016)] DOI: 10.3390/rs8100847. *Remote Sensing*, *9*(10), 2–5. https://doi.org/10.3390/rs9101003

Baptist, F., Yoccoz, N. G., & Choler, P. (2010). Direct and indirect control by snow cover over decomposition in alpine tundra along a snowmelt gradient. *Plant and Soil*, *328*(1–2), 397–410. https://doi.org/10.1007/s11104-009-0119-6

Barichivich, J., Briffa, K., Myneni, R., Schrier, G., Dorigo, W., Tucker, C., … Melvin, T. (2014). Temperature and Snow-Mediated Moisture Controls of Summer Photosynthetic Activity in Northern Terrestrial Ecosystems between 1982 and 2011. *Remote Sensing*, *6*(2), 1390–1431. https://doi.org/10.3390/rs6021390

Beamish, A. L., Coops, N. C., Hermosilla, T., Chabrillat, S., & Heim, B. (2018). Monitoring pigment-driven vegetation changes in a low-Arctic tundra ecosystem using digital cameras: *Ecosphere*, *9*(2). https://doi.org/10.1002/ecs2.2123

Beamish, A. L., Nijland, W., Edwards, M., Coops, N. C., & Henry, G. H. R. (2016). Phenology and vegetation change measurements from true colour digital photography in high Arctic tundra. *Arctic Science*, *2*(2), 33–49. https://doi.org/10.1139/as-2014-0003

Beamish, A. L., Raynolds, M. K., Epstein, H., Frost, G. v., Macander, M. J., Bergstedt, H., …Wagner, J. (2020). Recent trends and remaining challenges for optical remote sensing of Arctic tundra vegetation: A review and outlook. *Remote Sensing of Environment*, *246*, 111872. https://doi.org/10.1016/j.rse.2020.111872

Bintanja, R., & Andry, O. (2017). Towards a rain-dominated Arctic. *Nature Climate Change*, *7*(4), 263–267. https://doi.org/10.1038/nclimate3240

Bjorkman, A. D., Elmendorf, S. C., Beamish, A. L., Vellend, M., & Henry, G. H. R. (2015). Contrasting effects of warming and increased snowfall on Arctic tundra plant phenology over the past two decades. *Global Change Biology*, *21*(12), 4651–4661. https://doi.org/10.1111/gcb.13051

Bjorkman, A. D., Myers-Smidt, I. H., & Elmendorf, S. C. (2018). Plant functional trait change across a warming tundra biome. *Nature*, *562*, 57–81. https://doi.org/10.1038/s41586-018-0563-7

Bokhorst, S., Pedersen, S. H., Brucker, L., Anisimov, O., Bjerke, J. W., Brown, … Callaghan, T. V. (2016). Changing Arctic snow cover: A review of recent developments and assessment of future needs for observations, modelling, and impacts. *Ambio*, *45*(5), 516–537. https://doi.org/10.1007/s13280-016-0770-0

Brooks, M. E., Kristensen, K., van Benthem, K. J., Magnusson, A., Berg, C. W., Nielsen, A., … Bolker, B. M. (2017). {glmmTMB} Balances Speed and Flexibility Among Packages for Zero-inflated Generalized Linear Mixed Modeling. *The R Journal*, *9*(2), 378–400.

Callaghan, T. V., Johansson, M., Brown, R. D., Groisman, P. Ya., Labba, N., … Wood, E. F. (2011). Multiple Effects of Changes in Arctic Snow Cover. *Ambio*, *40*(S1), 32–45. https://doi.org/10.1007/s13280-011-0213-x

Christiansen, C. T., Lafreniére, M. J., Henry, G. H. R., & Grogan, P. (2018). Long-term deepened snow promotes tundra evergreen shrub growth and summertime ecosystem net CO2 gain but reduces soil carbon and nutrient pools. *Global Change Biology*, *24*(8), 3508–3525. https://doi.org/10.1111/GCB.14084

Constable, A.J., S. Harper, J. Dawson, K. Holsman, T. Mustonen, D. Piepenburg, and B. Rost, 2022: Cross-Chapter Paper 6: Polar Regions. In: *Climate Change 2022: Impacts, Adaptation, and Vulnerability.* Contribution of Working Group II to the Sixth Assessment Report of the Intergovernmental Panel on Climate Change [H.-O. Pörtner, D.C. Roberts, M. Tignor, E.S. Poloczanska, K. Mintenbeck, A. Alegría, M. Craig, S. Langsdorf, S. Löschke, V. Möller, A. Okem, B. Rama (eds.)]. Cambridge University Press. In Press.

Cooper, E. J. (2014). Warmer shorter winters disrupt arctic terrestrial ecosystems. *Annual Review of Ecology, Evolution, and Systematics*, *45*, 271–295. https://doi.org/10.1146/annurev-ecolsys-120213-091620

Cooper, E. J., Dullinger, S., & Semenchuk, P. (2011). Late snowmelt delays plant development and results in lower reproductive success in the High Arctic. *Plant Science*, *180*(1), 157–167. https://doi.org/10.1016/j.plantsci.2010.09.005

Cooper, E. J., Little, C. J., Pilsbacher, A. K., & Mörsdorf, M. A. (2019). Disappearing green: Shrubs decline and bryophytes increase with nine years of increased snow accumulation in the High Arctic. *Journal of Vegetation Science*, *30*(5), 857–867. https://doi.org/10.1111/jvs.12793

Cornelissen, J. H. C., Callaghan, T. V., Alatalo, J. M., Michelsen, A., Graglia, E., Hartley, A. E., … Aerts, R. (2001). Global change and arctic ecosystems: is lichen decline a function of increases in vascular plant biomass? *Journal of Ecology*, *89*(6), 984–994. https://doi.org/10.1111/J.1365-2745.2001.00625.X

Crawford, R. M. M., Chapman, H. M., & Hodge, H. (1994). Anoxia Tolerance in High Arctic Vegetation. *Arctic and Alpine Research*, *26*(3), 308–312. https://doi.org/10.1080/00040851.1994.12003071

Damgaard, C. F., & Irvine, K. M. (2019). Using the beta distribution to analyse plant cover data. *Journal of Ecology*, *107*(6), 2747–2759. https://doi.org/10.1111/1365-2745.13200

Edwards, A. C., Scalenghe, R., & Freppaz, M. (2007). Changes in the seasonal snow cover of alpine regions and its effect on soil processes: A review. *Quaternary International*, *162–163*, 172–181. https://doi.org/10.1016/j.quaint.2006.10.027

Ellebjerg, S. M., Tamstorf, M. P., Illeris, L., Michelsen, A., & Hansen, B. U. (2008). Inter-annual variability and controls of plant phenology and productivity at Zackenberg. *Advances in Ecological Research*, *40*, 249–273.

Elmendorf, S. C., Henry, G. H. R., Hollister, R. D., Björk, R. G., Bjorkman, A. D., Callaghan, T. V., … Wookey, P. A. (2012). Global assessment of experimental climate warming on tundra vegetation: Heterogeneity over space and time. *Ecology Letters*, *15*(2), 164–175. https://doi.org/10.1111/j.1461-0248.2011.01716.x

Elvebakk, A. (2005). A vegetation map of Svalbard on the scale 1:3.5 mill. *Phytocoenologia*, *35*(4), 951–967. https://doi.org/10.1127/0340-269X/2005/0035-0951

Engstrom, R., Hope, A., Kwon, H., & Stow, D. (2008). The Relationship Between Soil Moisture and NDVI Near Barrow, Alaska. *Physical Geography*, *29*(1), 38–53. https://doi.org/10.2747/0272-3646.29.1.38

Epstein, H. E., Walker, M. D., Stuart Chapin, F., & Starfield, A. M. (2000). A transient, nutrient-based model of Arctic plant community response to climate warming. *Ecological Applications*, *10*(3), 824–841. https://doi.org/10.1890/1051-0761

Faith, D. P., Minchin, P. R., Belbin, L. (1987). Compositional dissimilarity as a robust measure of ecological distance. *Vegetatio*, *69*, 57–68.

Hanssen-Bauer, I., Førland, E. J., Hisdal, H., Mayer, S., Sandø, A. B., & Sorteberg, A. (2019). Climate in Svalbard 2100 - a knowledge base for climate adaptation. *NCCS Report*, *2387–3027*(1/2019). http://www.miljodirektoratet.no/M1242

Happonen, K., Aalto, J., Kemppinen, J., Niittynen, P., Virkkala, A. M., & Luoto, M. (2019). Snow is an important control of plant community functional composition in oroarctic tundra. *Oecologia*, *191*(3), 601–608. https://doi.org/10.1007/s00442-019-04508-8

Hartig, F. (2021). DHARMa: Residual Diagnostics for Hierarchical (Multi-Level / Mixed) Regression Models. R package version 0.4.5. https://cran.r-project.org/package=DHARMa

Hijmans, R. J. (2022). raster: Geographic Data Analysis and Modeling. R package version 3.5-15. https://cran.r-project.org/package=raster

Johansson, M., Callaghan, T. v., Bosiö, J., Åkerman, H. J., Jackowicz-Korczynski, M., & Christensen, T. R. (2013). Rapid responses of permafrost and vegetation to experimentally increased snow cover in sub-arctic Sweden. *Environmental Research Letters*, *8*(3). https://doi.org/10.1088/1748-9326/8/3/035025

Karlsen, S. R., Anderson, H. B., van der Wal, R., & Hansen, B. B. (2018). A new NDVI measure that overcomes data sparsity in cloud-covered regions predicts annual variation in ground-based estimates of high arctic plant productivity. *Environmental Research Letters*, *13*(2), 025011. https://doi.org/10.1088/1748-9326/aa9f75

Kemppinen, J., Niittynen, P., Aalto, J., le Roux, P. C., & Luoto, M. (2019). Water as a resource, stress and disturbance shaping tundra vegetation. *Oikos*, *128*(6), 811–822. https://doi.org/10.1111/OIK.05764

Klanderud, K., & Totland, Ø. (2005). Simulated climate change altered dominance hierachies and diversity of an alpine biodiversity hotspot. *Ecology*, *86*(8), 2047–2054. https://doi.org/10.1890/04-1563

Leffler, A. J., Klein, E. S., Oberbauer, S. F., & Welker, J. M. (2016). Coupled long-term summer warming and deeper snow alters species composition and stimulates gross primary productivity in tussock tundra. *Oecologia*, *181*(1), 287–297. https://doi.org/10.1007/S00442-015-3543-8/FIGURES/5

Legendre, P., & Anderson, M. J. (1999). Distance-based Redudancy Analysis: Testing Multispecies Responses in Multifactorial Ecological Experiments. *Ecological Monographs*, *69*(1), 1–24.

Legendre, P., & Legendre, L. (2012). *Numerical ecology*. Elsevier.

Lemke, P., Ren, J., Alley, R. B., Allison, I., Carrasco, J., Flato, G., Fujii, Y., Kaser, G., Mote, P., Thomas, R. H., & others. (2007). *Observations: changes in snow, ice and frozen ground*.

Mark, A. F., Korsten, A. C., Guevara, D. U., Dickinson, K. J. M., Humar-Maegli, T., Michel, P., … Nielsen, J. A. (2015). Ecological Responses to 52 Years of Experimental Snow Manipulation in High-Alpine Cushionfield, Old Man Range, South-Central New Zealand. *Arctic, Antarctic, and Alpine Research*, *47*(4), 751–772. https://doi.org/10.1657/AAAR0014-098

Martin, A. C., Jeffers, E. S., Petrokofsky, G., Myers-Smith, I., & MacIas-Fauria, M. (2017). Shrub growth and expansion in the Arctic tundra: an assessment of controlling factors using an evidence-based approach. *Environmental Research Letters*, *12*(8), 085007. https://doi.org/10.1088/1748-9326/AA7989

May, J. L., & Beamish, A. L. (2015). The Contribution of Moss to Plot-Based Spectral Signals in Moist Acidic Low Arctic Tundra. *American Geophysical Union, Fall Meeting Abstracts*. https://ui.adsabs.harvard.edu/abs/2015AGUFM.B31C0563M/abstract

May, J. L., Parker, T., Unger, S., & Oberbauer, S. F. (2018). Short term changes in moisture content drive strong changes in Normalized Difference Vegetation Index and gross primary productivity in four Arctic moss communities. *Remote Sensing of Environment*, *212*, 114–120. https://doi.org/10.1016/j.rse.2018.04.041

Morgner, E., Elberling, B., Strebel, D., & Cooper, E. J. (2010). The importance of winter in annual ecosystem respiration in the High Arctic: effects of snow depth in two vegetation types. *Polar Research*, *29*(1), 58–74. https://doi.org/10.1111/j.1751-8369.2010.00151.x

Moriana-Armendariz, M., Abbandonato, H., Yamaguchi, T., Mörsdorf, M. A., Aares, K. H., Semenchuk, P. R., … Cooper, E. J. (2021). Increased snow and cold season temperatures alter High Arctic parasitic fungi – host plant interactions. *Arctic Science*, 1–27. https://doi.org/10.1139/as-2020-0027

Mörsdorf, M. A., Baggesen, N. S., Yoccoz, N. G., Michelsen, A., Elberling, B., Ambus, P. L., & Cooper, E. J. (2019). Deepened winter snow significantly influences the availability and forms of nitrogen taken up by plants in High Arctic tundra. *Soil Biology and Biochemistry*, *135*, 222–234. https://doi.org/10.1016/j.soilbio.2019.05.009

Mörsdorf, M. A., & Cooper, E. J. (2021). Habitat determines plant community responses to climate change in the High Arctic. *Arctic Science*, 1–22. https://doi.org/10.1139/as-2020-0054

Myers-Smith, I. H., Kerby, J. T., Phoenix, G. K., Bjerke, J. W., Epstein, H. E., Assmann, J. J., … Wipf, S. (2020). Complexity revealed in the greening of the Arctic. *Nature Climate Change*, *10*(2), 106–117. https://doi.org/10.1038/s41558-019-0688-1

Natali, S. M., Schuur, E. A. G., & Rubin, R. L. (2012). Increased plant productivity in Alaskan tundra as a result of experimental warming of soil and permafrost. *Journal of Ecology*, *100*(2), 488–498. https://doi.org/10.1111/J.1365-2745.2011.01925.X

Niittynen, P., Heikkinen, R. K., Aalto, J., Guisan, A., Kemppinen, J., & Luoto, M. (2020). Fine-scale tundra vegetation patterns are strongly related to winter thermal conditions. *Nature Climate Change 2020 10:12*, *10*(12), 1143–1148. https://doi.org/10.1038/s41558-020-00916-4

Niittynen, P., Heikkinen, R. K., & Luoto, M. (2018). Snow cover is a neglected driver of Arctic biodiversity loss. *Nature Climate Change*, *8*(11), 997–1001. https://doi.org/10.1038/s41558-018-0311-x

Niittynen, P., & Luoto, M. (2018). The importance of snow in species distribution models of arctic vegetation. *Ecography*, *41*(6), 1024–1037. https://doi.org/10.1111/ecog.03348

Oksanen, J., Blanchet, F. G., Friendly, M., Kindt, R., Legendre, P., McGlinn, D., … Wagner, H. (2020). vegan: Community Ecology Package. R package version 2.5-7. https://cran.r-project.org/package=vegan

Pan, N., Feng, X., Fu, B., Wang, S., Ji, F., & Pan, S. (2018). Increasing global vegetation browning hidden in overall vegetation greening: Insights from time-varying trends. *Remote Sensing of Environment*, *214*, 59–72. https://doi.org/10.1016/J.RSE.2018.05.018

Parmentier, F. J. W., Nilsen, L., Tømmervik, H., & Cooper, E. J. (2021). A distributed time-lapse camera network to track vegetation phenology with high temporal detail and at varying scales. *Earth System Science Data*, *13*(7), 3593–3606. https://doi.org/10.5194/essd-13-3593-2021

Parmentier, F. J. W., Nilsen, L., Tømmervik, H., Meisel, O. H., Bröder, L. M., Vonk, J. E., … Cooper, E. J. (2019). Thicker Snow Cover Triggers Permafrost Carbon Loss Through Both Enhanced Warming and Surface Runoff. *Geophysical Research Abstracts*, *21*.

Pattison, R. R., & Welker, J. M. (2014). Differential ecophysiological response of deciduous shrubs and a graminoid to long-term experimental snow reductions and additions in moist acidic tundra, Northern Alaska. *Oecologia*, *174*(2), 339–350. https://doi.org/10.1007/S00442-013-2777-6/FIGURES/4

Peter, J. S., Hogland, J., Hebblewhite, M., Hurley, M. A., Hupp, N., & Proffitt, K. (2018). Linking phenological indices from digital cameras in Idaho and Montana to MODIS NDVI. *Remote Sensing*, *10*(10), 1–15. https://doi.org/10.3390/rs10101612

Richardson, A. D. (2019). Tracking seasonal rhythms of plants in diverse ecosystems with digital camera imagery. *New Phytologist*, *222*(4), 1742–1750. https://doi.org/10.1111/NPH.15591

Rixen, C., Høye, T. T., Macek, P., Aerts, R., Alatalo, J. M., Anderson, J. T., … Zong, S. (2022). Winters are changing: snow effects on Arctic and alpine tundra ecosystems. *Arctic Science*, 1–37. https://doi.org/10.1139/as-2020-0058

RStudio Team. (2022). RStudio: Integrated Development Environment for R (2022.2.0.443). RStudio, PBC, Boston, MA, USA. http://www.rstudio.com/

Rumpf, S. B., Semenchuk, P. R., Dullinger, S., & Cooper, E. J. (2014). Idiosyncratic responses of high arctic plants to changing snow regimes. *PLoS ONE*, *9*(2). https://doi.org/10.1371/journal.pone.0086281

Saccone, P., Hoikka, K., & Virtanen, R. (2017). What if plant functional types conceal species-specific responses to environment? Study on arctic shrub communities. *Ecology*, *98*(6), 1600–1612. https://doi.org/10.1002/ECY.1817

Schimel, J. P., Bilbrough, C., & Welker, J. M. (2004). Increased snow depth affects microbial activity and nitrogen mineralization in two Arctic tundra communities. *Soil Biology and Biochemistry*, *36*(2), 217–227. https://doi.org/10.1016/J.SOILBIO.2003.09.008

Semenchuk, P. R., Elberling, B., Amtorp, C., Winkler, J., Rumpf, S., Michelsen, A., & Cooper, E. J. (2015). Deeper snow alters soil nutrient availability and leaf nutrient status in high Arctic tundra. *Biogeochemistry*, *124*(1–3), 81–94. https://doi.org/10.1007/s10533-015-0082-7

Semenchuk, P. R., Gillespie, M. A. K., Rumpf, S. B., Baggesen, N., Elberling, B., & Cooper, E. J. (2016). High Arctic plant phenology is determined by snowmelt patterns but duration of phenological periods is fixed: An example of periodicity. *Environmental Research Letters*, *11*(12), 1–12. https://doi.org/10.1088/1748-9326/11/12/125006

Sjögersten, S., Kuijper, D. P. J., van der Wal, R., Loonen, M. J. J. E., Huiskes, A. H. L., & Woodin, S. J. (2010). Nitrogen transfer between herbivores and their forage species. *Polar Biology*, *33*(9), 1195–1203. https://doi.org/10.1007/S00300-010-0809-9/FIGURES/3

Smithson, M., & Verkuilen, J. (2006). A better lemon squeezer? Maximum-likelihood regression with beta-distributed dependent variables. *Psychological Methods*, *11*(1), 54–71. https://doi.org/10.1037/1082-989X.11.1.54

Tømmervik, H., Karlsen, S.-R., Nilsen, L., Johansen, B., Storvold, R., Zmarz, A., … Bjerke, J. W. (2014). Use of unmanned aircraft systems (UAS) in a multi-scale vegetation index study of arctic plant communities in Adventdalen on Svalbard. *EARSeL EProceedings, Special Issue: 34 th EARSeL Symposium*. https://hdl.handle.net/10037/6651

Valøen, K. (2019). *Stochastic rain events increase NDVI through moss water content: a HighArctic field experiment*. NTNU - Norwegian University of Life Sciences.

van der Wal, R., & Brooker, R. W. (2004). Mosses mediate grazer impacts on grass abundance in arctic ecosystems. *Functional Ecology*, *18*(1), 77–86. https://doi.org/10.1111/J.1365-2435.2004.00820.X

Vittoz, P., & Guisan, A. (2007). How reliable is the monitoring of permanent vegetation plots? A test with multiple observers. *Journal of Vegetation Science*, *18*(3), 413–422. https://doi.org/10.1111/j.1654-1103.2007.tb02553.x

Wahren, C. H. A., Walker, M. D., & Bret-Harte, M. S. (2005). Vegetation responses in Alaskan arctic tundra after 8 years of a summer warming and winter snow manipulation experiment. *Global Change Biology*, *11*(4), 537–552. https://doi.org/10.1111/J.1365-2486.2005.00927.X

Westergaard-Nielsen, A., Lund, M., Hansen, B. U., & Tamstorf, M. P. (2013). Camera derived vegetation greenness index as proxy for gross primary production in a low Arctic wetland area. *ISPRS Journal of Photogrammetry and Remote Sensing*, *86*, 89–99. https://doi.org/10.1016/j.isprsjprs.2013.09.006

Westergaard-Nielsen, A., Lund, M., Pedersen, S. H., Schmidt, N. M., Klosterman, S., Abermann, J., & Hansen, B. U. (2017). Transitions in high-Arctic vegetation growth patterns and ecosystem productivity tracked with automated cameras from 2000 to 2013. *Ambio*, *46*(s1), 39–52. https://doi.org/10.1007/s13280-016-0864-8

Wijk, S. (1986). Performance of Salix Herbacea in an Alpine Snow-Bed Gradient. *The Journal of Ecology*, *74*(3), 675. https://doi.org/10.2307/2260390

Wipf, S., & Rixen, C. (2010). A review of snow manipulation experiments in Arctic and alpine tundra ecosystems. *Polar Research*, *29*(1), 95–109. https://doi.org/10.1111/j.1751-8369.2010.00153.x

Xiaoqin, W., Miaomiao, W., Shaoqiang, W., & Yundong, W. (2015). Extraction of vegetation information from visible unmanned aerial vehicle images. *Transactions of the Chinese Society of Agricultural Engineering*, *31*(5).

Xu, W., Prieme, A., Cooper, E. J., Mörsdorf, M. A., Semenchuk, P., Elberling, B., … Ambus, P. L. (2021). Deepened snow enhances gross nitrogen cycling among Pan-Arctic tundra soils during both winter and summer. *Soil Biology and Biochemistry*, *160*. https://doi.org/10.1016/j.soilbio.2021.108356

Xue, J., & Su, B. (2017). Significant Remote Sensing Vegetation Indices: A Review of Developments and Applications. *Journal of Sensors*, *2017*, 1–17. https://doi.org/10.1155/2017/1353691

Zarco-Tejada, P. J., González-Dugo, V., & Berni, J. A. J. (2012). Fluorescence, temperature and narrow-band indices acquired from a UAV platform for water stress detection using a micro-hyperspectral imager and a thermal camera. *Remote Sensing of Environment*, *117*, 322–337. https://doi.org/10.1016/J.RSE.2011.10.007

Zuur, A. F., & Ieno, E. N. (2016). A protocol for conducting and presenting results of regression-type analyses. *Methods in Ecology and Evolution*, *7*(6), 636–645. https://doi.org/10.1111/2041-210X.12577

Zuur, A. F., Ieno, E. N., & Elphick, C. S. (2010). A protocol for data exploration to avoid common statistical problems. *Methods in Ecology and Evolution*, *1*(1), 3–14. https://doi.org/10.1111/j.2041-210x.2009.00001.x

Supplementary material

Figure 13. Soil collapse after possible melt-out of an ice lens behind snow fence C7. Agnes Nielsen preparing to survey a vegetation plot. Photograph taken in July 2021 by myself.

Table S1. Forward model selection for constraining model in distance-based redundancy analysis (dbRDA) on plant community response to Snow regime (Ambient/Deep) and Year (2015, 2020, 2021). An Akaike Information Criteria (AIC)-like criteria based on chi-squares, adjusted R2 and p-values are given for each added model term based on permutation tests (999 permutations). The model with the lowest AIC is the most parsimonious model 'Snow regime' and 'Year' are treated as constraining variables while 'Fence' and Dominant Evergreen Shrub ('DES') are treated as conditioning variables. Interactions between variables are indicated with 'X'.

Reference model	Added term	AIC	R^2 (adjusted)	p-value
[species x cover] ~ 1				
	+ Snow regime	1181.2	0.142	0.001
	+ Year	1207.0	0.0304	0.001
	+ cond(Fence + DES)	1147.4	0.000	
[species x cover] ~ Snow regime		1181.2	0.142	
	+ Year	1176.5	0.174	0.001
	+ cond(Fence + DES)	1100.0	0.163	
[species x cover] ~ Snow regime + Year		1176.5	0.199	
	+ Snow regime × year	1177.8	0.179	0.149
	+ cond(Fence + DES)	1090.8	0.190	

Table S2. Plots used in 2015, 2020, and 2021 listed by plot IDs. In 2015, 39 plots were used while the same 123 plots were used in 2020 and 2021. Prefixes including capital letters A-D and number 1-12 refer to snow fence locations where letters indicate which block a fence belongs to, and numbers give each fence a unique ID. Letters 'N' and 'H' refer to 'Ambient' and 'Deep' snow, respectively. Suffixes including capital letters 'D' or 'C' and a number between 1-3 refer to 'Dominant Evergreen Shrub (DES)' where D: Dryas and C: Cassiope. Numbers 1-3 give each plot a unique ID.

2015	2020	2020 continued	2020 continued	2021	2021 continued	20201 continued
A1NC3	A1NC1	B5ND3	C9HC1	A1NC1	B5ND3	C9HC1
A1ND3	A1NC2	B5HC1	C9HC2	A1NC2	B5HC1	C9HC2
A1HC1	A1NC3	B5HC2	C9HC3	A1NC3	B5HC2	C9HC3
A1HD1	A1ND1	B5HC3	C9HD1	A1ND1	B5HC3	C9HD1
A3NC1	A1ND2	B5HD1	C9HD2	A1ND2	B5HD1	C9HD2
A3ND1	A1ND3	B5HD2	C9HD3	A1ND3	B5HD2	C9HD3
A3HC1	A1HC1	B5HD3	D10NC1	A1HC1	B5HD3	D10NC1
A3HD2	A1HC2	B6NC1	D10NC2	A1HC2	B6NC1	D10NC2
B4NC1	A1HC3	B6NC2	D10NC3	A1HC3	B6NC2	D10NC3
B4ND1	A1HD1	B6NC3	D10ND1	A1HD1	B6NC3	D10ND1
B4HC3	A1HD2	B6ND1	D10ND2	A1HD2	B6ND1	D10ND2
B5NC3	A1HD3	B6ND2	D10ND3	A1HD3	B6ND2	D10ND3
B5ND2	A3NC1	B6ND3	D10HC1	A3NC1	B6ND3	D10HC1
B5HC1	A3NC2	B6HC1	D10HC2	A3NC2	B6HC1	D10HC2
B5HD1	A3NC3	B6HC2	D10HC3	A3NC3	B6HC2	D10HC3
B6NC3	A3ND1	B6HC3	D10HD2	A3ND1	B6HC3	D10HD2
B6ND2	A3ND2	B6HD1	D10HD3	A3ND2	B6HD1	D10HD3
B6HC1	A3ND3	B6HD2	D11NC1	A3ND3	B6HD2	D11NC1
B6HD3	A3HC1	B6HD3	D11NC2	A3HC1	B6HD3	D11NC2
C8NC3	A3HC2	C7NC1	D11NC3	A3HC2	C7NC1	D11NC3
C8ND1	A3HC3	C7NC2	D11ND1	A3HC3	C7NC2	D11ND1
C8HD1	A3HD1	C7NC3	D11ND2	A3HD1	C7NC3	D11ND2
C9NC2	A3HD2	C7ND1	D11ND3	A3HD2	C7ND1	D11ND3
C9ND2	A3HD3	C7ND2	D11HC1	A3HD3	C7ND2	D11HC1
C9HC1	B4NC1	C7ND3	D11HC2	B4NC1	C7ND3	D11HC2
C9HD1	B4NC2	C7HD1	D11HC3	B4NC2	C7HD1	D11HC3
D10NC1	B4NC3	C8NC1	D11HD1	B4NC3	C8NC1	D11HD1
D10ND1	B4ND1	C8NC2	D11HD2	B4ND1	C8NC2	D11HD2
D10HC2	B4ND2	C8NC3	D11HD3	B4ND2	C8NC3	D11HD3
D10HD1	B4ND3	C8ND1	D12NC1	B4ND3	C8ND1	D12NC1
D11NC1	B4HC1	C8ND2	D12NC2	B4HC1	C8ND2	D12NC2
D11ND1	B4HC2	C8ND3	D12NC3	B4HC2	C8ND3	D12NC3
D11HC1	B4HC3	C8HD1	D12ND1	B4HC3	C8HD1	D12ND1
D11HD1	B4HD1	C8HD2	D12ND2	B4HD1	C8HD2	D12ND2
D12NC1	B4HD2	C8HD3	D12ND3	B4HD2	C8HD3	D12ND3
D12ND3	B4HD3	C9NC1	D12HC1	B4HD3	C9NC1	D12HC1
D12HC2	B5NC1	C9NC2	D12HC2	B5NC1	C9NC2	D12HC2
D12HD2	B5NC2	C9NC3	D12HC3	B5NC2	C9NC3	D12HC3
	B5NC3	C9ND1	D12HD1	B5NC3	C9ND1	D12HD1
	B5ND1	C9ND2	D12HD2	B5ND1	C9ND2	D12HD2
	B5ND2	C9ND3	D12HD3	B5ND2	C9ND3	D12HD3